université paris – sud
INSTITUT DE PHYSIQUE NUCLEAIRE
B.P. N° 1 : 91406 - ORSAY TEL. 941.51.10
laboratoire associé à l'IN2 P3

FR8002822

High-Lying Neutron Hole strengths observed in pick-up reactions

---

Sydney Galès

Institut de Physique Nucléaire,
B.P. n°1, 91406 Orsay, France

Invited talk at the International Conference on Nuclear Physics

August 23-30 1980,
Berkeley, California, U.S.A.

IPNPhN 80-23

HIGH-LYING NEUTRON HOLE STRENGTHS OBSERVED IN PICK-UP REACTIONS

Sydney Gales

Institut de Physique Nucleaire, BP nº 1, 91406
Orsay Cedex, France

Abstract: Neutron-hole states in orbits well below the Fermi surface have been observed in a number of medium-heavy nuclei from A=90 to 209 using one nucleon pick-up reactions. The excitation energies, angular distributions of such broad and enhanced structures will be discussed. The fragmentation of the neutron-hole strengths as well as the spreading of such simple mode of excitations into more complex states are compared to recent calculations within the quasiparticle-phonon or the single particle-vibration coupling nuclear models. We report on recent measurements of J for inner-hole states in ^{89}Zr and ^{115,119}Sn using the analyzing power of the ($\vec{p}$,d) and ($\vec{d}$,t) reactions. Large enhancement of cross-sections are observed at high excitation energy in the study of the (p,t) reactions on Zr, Cd, Sn, Te and Sm isotopes. The systematic features of such high-lying excitation are related to the ones observed in one neutron pick-up experiments. The origin of such concentration of two neutron-hole strengths in Cd and Sn isotopes will be discussed. Preliminary results obtained in the study of the (α,^{6}He) reaction at 218 MeV incident energy on ^{90}Zr, ^{118}Sn and ^{208}Pb targets are presented and compared to the (p,t) results. Finally the properties of hole-analog states populated in neutron pick-up reactions (from ^{90}Zr to ^{208}Pb) will be presented.

1. Introduction

Studies of one nucleon transfer reactions to orbits near the Fermi surface have established that, to a good approximation, nucleons inside the nucleus move independently in an average potential. When one comes to study high-lying states, e.g. inner-hole states well below the Fermi surface, one can expect interesting features showing deviations from bare single-particle properties. The state density increases and the structure of nuclear levels becomes more complicated with increasing excitation energy. Under such conditions, one would like to examine the behaviour of a number of simple excitation modes of the nucleus. Many examples of such simple structures, such as multipole giant resonances, isobaric analog states, one or two holes states, and more recently giant "spin-flip" resonances are under study using a variety of nuclear reactions. In this field "light" ions beams (p,d,^{3}He and α) in the energy range of 40 to 200 MeV have turned out to be quite successful in probing such high-lying excitations of the nucleus.

The examples which I shall discuss in this paper are the hole-states observed at high excitation energy (4 to 15 MeV) in one and two nucleons pick-up reactions on target nuclei ranging from ^{90}Zr to ^{209}Bi. I would like to only summarize this work since recent reports on these questions have been given recently.[1])

The investigation of the deeply-bound states in nuclei were thought for a long time to be limited to light nucleon systems. The extensive studies of the (p,2p) knock-out reactions[2]), supported later by the (e,e'p) experiments[3]) have established the usefulness of

the shell model picture for nuclei up to ^{40}Ca-^{58}Ni. When one comes to heavier nuclei, these approaches are not easily applicable both for experimental reasons (coincidence yield and energy resolution) and because of the structure of the nucleus. In Fig. 1a a schematic representation of the nuclear well for two nuclei ^{28}Si and ^{208}Pb is presented. The radius of the well increases like $A^{1/3}$ whereas the potential depth remains rather constant when one goes from ^{28}Si to ^{208}Pb. However in the case of ^{208}Pb, one has to fill up the well with many more orbitals leading to very closely spaced subshells as opposed to the ^{28}Si case. On the other hand, due to the residual interactions which will mix the pure single-hole states with the high density of 2h-1p levels as represented in Fig. 1b, the inner-hole states will overlap leading to broad structure in the energy spectra of the residual nucleus.

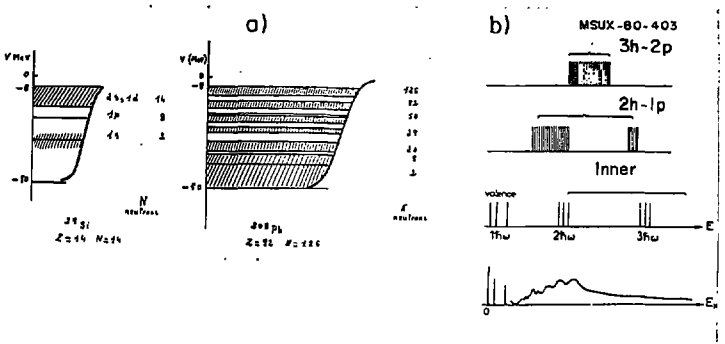

Fig. 1. (a) Schematic representation of the nuclear potential for A=28 and A=208
(b) Schematic representation of the valence, inner hole states in a nucleus and of the density of more complex states (2h-1p) and (3h-2p). The lower figure is obtained when one switchs on the residual interaction.

In the next section, I shall discuss the one neutron pick-up data on different isotope chains and its connection with the collectives properties of the target nucleus. The theoretical predictions for the response function of a hole-state to high excitation energy will be compared with experimental results. In section 3, recent measurements of analyzing powers in the study of the (p,d) and (d,t) reactions on Zr and Sn targets will be presented. The systematic features of the two nucleon pickup data at different incident energy and preliminary comparison between the (p,t) and the (α,^{6}He) reactions to high-lying states will be discussed in section 4.

It is also well known that one neutron pick-up experiments excite both components of the isospin doublet ($T_< = T_0 - 1$ and $T_> = T_0 + 1$) when T_0 is the isospin of the target. In view of the large amount of new experimental data accumulated in the last five years on hole-analog states ($T_>$ configurations) and their close connection with the inner-hole strengths in nuclei ($T_<$ states), the properties of such high-lying levels will be considered in section 5. Finally some conclusions will be drawn in section 6.

2. Inner-holes states observed in one neutron pick-up experiments

Since the initial observation of deep-hole states in (p,d) reactions by Sakai and Kubo,[4] neutron pick-up reactions have been widely used to study high-lying neutron-hole strenghts in medium-heavy nuclei. They have been observed in (p,d), (d,t) and (^{3}He,α) reactions at various energies from mass 90 to mass 209.[5-18]

Similarly proton-hole states corresponding to inner shells have been populated via the (d,^{3}He) reaction on ^{144,148,152}Sm and ^{90}Zr targets.[19-20]). Spectra from the (p,d) and (^{3}He,α) reaction on a number of target nuclei are displayed in fig. 2. These data were taken respectively at 42 MeV for the (p,d) reaction and at 70 MeV for the (^{3}He,α) case using the Michigan State University K=50 Isochronous Cyclotron. A number of common features are observed in the spectra of fig. 2 and they are typical of the results obtained in the study of neutron pick-up reactions to inner-hole states. Above the well resolved low-lying states, the residual spectra exhibits rather strong excitations of group of states or gross structure peaks riding on a continuous background. The energy spacing between the "giant-resonance" like structure and the low-lying levels is in general larger for nuclei near closed shells. Moreover some "fine-structure" peaks could be observed in some cases (^{89}Zr,^{111,117}Sn,^{207}Pb) whereas a broad bump with a high energy tail is present in the Te and Sm spectra. Before dealing with the nuclear structure information which one can extract from the systematics of the existing data, I would like to briefly describe the experimental procedure and the reaction model used in the data analysis.

2.1 EXPERIMENTAL PROCEDURE AND REACTION ANALYSIS

2.1.1 Experimental procedure

As one probes deeper in the nucleus, both high incident energy and a large range of excitation energy are required. In the spectra of fig. 2, the explored region was about 28 MeV for the (^{3}He,α) experiments and 10 to 14 MeV for the (p,d) studies. This was accomplished using a 50 cm gas delay-line counter backed by a plastic scintillator placed at the focal plane of a split-pole spectrometer. Such a detection system ensures a clean identification of the emitted particles and allows measurements at very forward angles (to 2°5 lab angle). In order to extract the cross-sections of the high-lying states a background subtraction has been made (see horizontal solid and dashed lines in fig. 2).

The energy resolution in the outgoing channel as well as the angular momentum matching conditions are two other very important parameters in view of the expected fragmentation and spreading of the inner-neutron hole strength in medium-heavy nuclei. If one carefully chooses the incident energy and the reaction, one could selectively enhance hole states with large (ℓ=4 to 6) or low (ℓ=1 to 2) angular

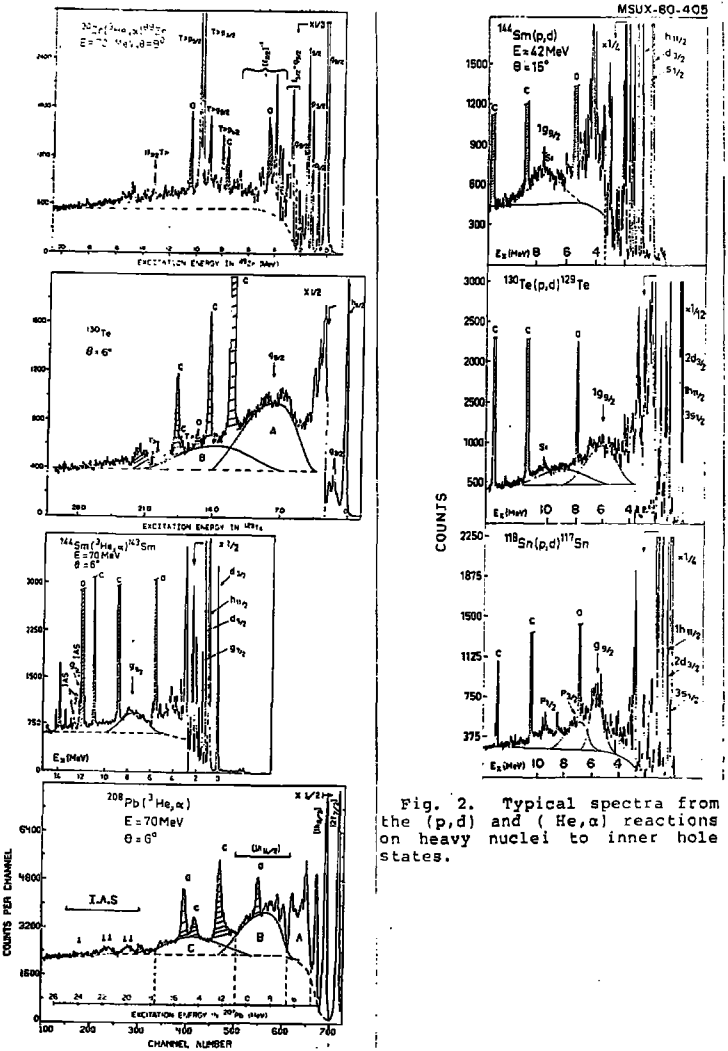

Fig. 2. Typical spectra from the (p,d) and (He,α) reactions on heavy nuclei to inner hole states.

momentum transfers. The best example of such an approach is in the tin isotopes where as many as seven measurements have been reported.[1,4-11,17] In all these experiments, a bump has been observed near 5.5 MeV excitation energy which is populated by a $\ell=4$ transfer. This narrow structure, identified with the $1g_{9/2}$ inner hole strength, is enhanced in the (^{3}He,α) studies whereas a broad side peak is only clearly observed in the (p,d) and (d,t) studies. These features are clearly present in the spectra of Fig. 3 obtained at MSU for the reactions ^{112,118}Sn(p,d)^{111,117}Sn at 42 MeV incident

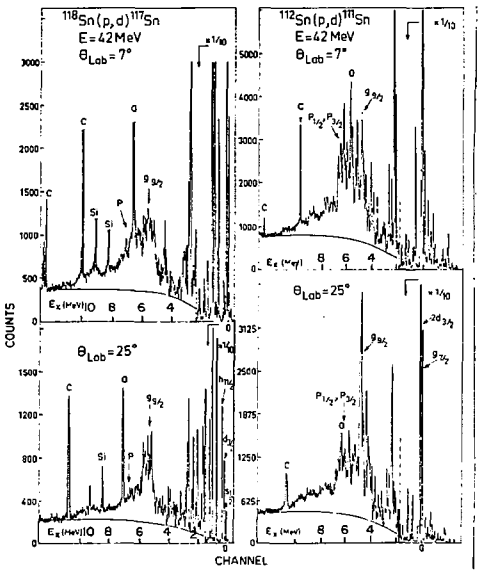

Fig. 3. Energy spectra from the reactions ^{112,118}Sn(p,d) at 42 MeV incident energy.

energy. The forward angle data enhances the $\ell=1$ component (labelled $p_{1/2}, p_{3/2}$ in Fig. 3) whereas in the spectra taken at $\theta=25$, one can clearly observe the narrow peak corresponding to the $\ell=4$ component. These spectra were obtained with an energy resolution of 25-30 keV and therefore one could see, especially in the case of ^{111}Sn, that the broad structure consists of a number of narrow peaks. The existence of such "fine structure" was first reported by the Orsay group using the (d,t) reaction with 18 keV energy resolution.[11] I would like to emphasize that only a careful analysis of each fragment

will allow an unambiguous determination of the centroid energy and spreading width of such high-lying excitation

2.1.2 Analysis

The experimental data have been compared to DWBA calculations performed with the code DWUCK.[21]) As a guide for our analysis, we have calculated the angular distributions for a number of low-lying states (from ^{89}Zr to ^{207}Pb) populated through various ℓ transfers (ℓ=0 to 6) either in the (^{3}He,α) or the (p,d) studies.

The analysis of all the 70 MeV (^{3}He,α) data was similar to the one reported in the study of the ^{208}Pb(^{3}He,α)^{207}Pb reaction.[16]) The optical potentials for both ^{3}He and α channels correspond to deep families ($V_{^3He}$=160 MeV,V_α=200 MeV) and similar set of parameters have been successfully used in the analysis of this reaction to hole states in Zr [15]) Sn[17]) and Pb[16,18]) isotopes. The calculations were made using the zero-range local approximation with a normalization constant of N=23.

In the case of the (p,d) reaction at 42 MeV, the Becchetti-Greenlees[23]) parameters were employed for the proton channel and the deuteron potential was deduced using the same set of results within the adiabatic approximation.[24]) Exact finite-range calculations were found to make very little difference for both the shape and the magnitude of the (p,d) cross-sections whereas the use of non-locality increases the quality of the fit to the experimental data.

Typical examples of the results of such analysis for various transfers and Q values are shown in figs. 4 and 5. Very good fits are obtained for both reactions allowing in general an anambiguous determination of the angular momentum transfer ℓ. The importance of the very forward angle data in the case of the (^{3}He,α) reaction is shown in fig. 4 (differences between ℓ and ℓ+1 transfers). Another check is the deduced spectroscopic strengths obtained from such analysis. Overall agreement is found between our results and the ones reported in previous studies of the low-lying hole states in medium heavy nuclei.

In view of the consistent analysis carried out for a wide range of nuclei the results obtained are quite satisfactory and give us some confidence in extending such an analysis to deeply-bound hole states. In order to make a qualitative comparison with nuclear models, one has to determine the lowest energy moments of the neutron-hole strength distributions for each orbital nℓJ

(i) the occupation number $N = \Sigma_i C^2S_i$ or observed amount of total strength, the upper limit being equal to 2J+1.

(ii) the centroid energy $\bar{E} = \Sigma_i E_i C^2S_i/N$. This quantity is related to the neutron binding energy.

(iii) the spreading width σ given by the relation
$\sigma^2 = \Sigma_i(\bar{E}-E_i)^2C^2S_i/N$

where C^2S_i is the fraction of the hole-strength in the fragment i at the excitation energy E_i. In performing such an analysis, one has to make the following assumptions which of course will limit the accuracy of the quantities E, N and σ.

(a) only ℓ transfers are determined in the study of transfer reactions. In many cases valence and inner holes belong to spin-orbit

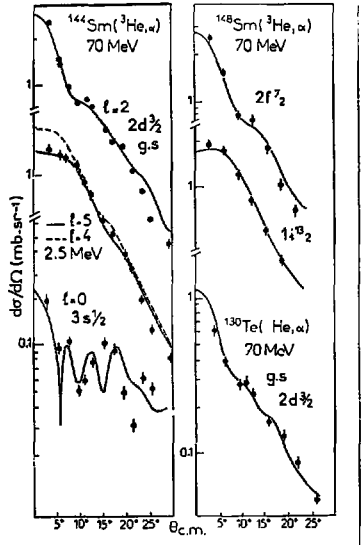

Fig. 4. Angular distributions for the low-lying states in ^{129}Te, ^{143,145,147}Sm populated in the (^{3}He,α) reaction. Solid curves are DWBA predictions. Reaction names and ℓ values are indicated in each case.

partners ($1f_{5/2}$ and $1f_{7/2}$ in Zr, $1g_{7/2}$ and $1g_{9/2}$ in Sn, Te, Sm, etc.,). Therefore one has to assume that the low-lying states (up to 3 MeV) correspond to the fragmentation of the valence orbits. Very recent polarization data for both valence and inner shells will help in clarifying this situation (see section 3).

(b) The explored energy range in the residual nucleus is limited to a maximum value E_o. Moreover, even high resolution experiments will be not able to separate the contributions coming from different subshells due to the high level density. These two factors will certainly limit our knowledge of the high energy tail of the hole strength distributions, and might lead to a centroid energy $\bar{E}$ which is shifted to low energy.

(c) The procedure adopted to extract C^2S values which is well established for strong hole components located near the Fermi level might be not applicable to highly fragmented deep-hole states. In particular the form-factor could be very different from the one deduced from the binding energy or separation energy methods. These effects have been evaluated in the case of inner-holes in ^{207}Pb by

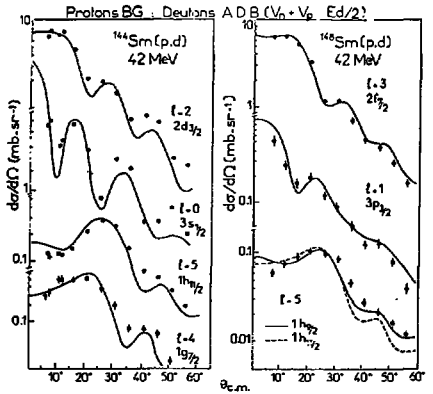

Fig. 5. Angular distributions for the low-lying states in ^{143,147}Sm populated in the (p,d) reaction. Solid curves are DWBA predictions for the indicated ℓ values.

comparing the spectroscopic strengths deduced using a Wood-Saxon form factor to those from Hartree-Fock calculations.[18]) Significant difference (up to 30%) have been found between the extracted C^2S values.

(d) Whereas the main part of the "giant-resonance" like structure is populated by a direct one-step process both low and high energy tails seem to contain large collective components (hole-phonon or core-polarized configurations).[17]) An estimate of the two-step process contribution to the $1g_{9/2}$ inner-hole strength in ^{115}Sn[17]) has been found to give results which differ by as much as 50% in the high energy tail of the neutron-hole distribution.

Taking into account these limitations, let us examine the results in various regions of the mass table.

2.2 NUCLEAR STRUCTURE INFORMATION AND COMPARISON WITH NUCLEAR MODELS

2.2.1 The Zr region (20<N<50)

One neutron-hole strength corresponding to the $1f_{7/2}$ inner shell has been observed in the $^{90}Zr(^3He,\alpha)^{89}Zr$ reaction[6,15,25] at 39, 100 and 205 MeV incident energy. High resolution work[15] has shown highly fragmented structure between 3.5 and 7.0 MeV excitation energy populated by an ℓ=3 transfer. The relevent structure information is summarized in Table 1 and compared to the H.F. calculations of Beiner and Lombard using a density-dependent force.[26]

Table 1. Centroid energies, widths and total strengths for inner-hole states in ^{89}Zr.

nℓJ	C^2Si/N	Γ=2.35σ (MeV)	$\tilde{E}$ (MeV)	E_{HF}[a] (MeV)	ε_{so}[b] (MeV) exp	theo
$1f_{7/2}$	0.5-0.7	2.23	5.20	8.80	3.0 5.1[c]	4.40
2s-1d		>5	~15.0	14.40		

a) Ref. 26.
b) Spin-orbit splitting for $f_{5/2}$-$f_{7/2}$ neutron orbitals. Theoretical values are from Ref. 26.
c) Spin-orbit splitting from proton-hole states in ^{89}Y. See Ref. 20.

Useful information is obtained especially for the spin-orbit splitting between $1f_{7/2}$ and $1f_{5/2}$ neutron orbitals. Similar results have been obtained for proton-hole orbits by Wagner et al.[20] The discrepancy between the quantities $\tilde{E}$ and E_{HF} might be greatly reduced if a better determination of the high energy tail of the $1f_{7/2}$ hole-strength were obtained.

High energy (p,d) data on ^{90}Zr have recently been reported[1] using the unpolarized and polarized beam of the Indiana University Cyclotron. A typical spectrum obtained at 90 MeV is shown in fig. 6. There is also an indication of additional broad structure under the region of the IAS (8-10 MeV) and around 15 MeV. Similar features are also present in the study of the ($^3He,\alpha$) reaction at 100 MeV and 130 MeV.[25] The highest part could possibly be attributed to pick-up from the next inner shell, 2s-1d shell. The results from the polarized beam experiments will be discussed in the next section.

2.2.2 The Cd, Sn and Te region (50<N<82)

As mentioned earlier inner hole-states in the Sn isotopes from A=111 to A=123 have been studied by many groups. A recent high resolution study of the ($^3He,\alpha$) reaction[17] has beautifully demonstrated the change of the fragmentation and the spreading of the

$lg_{9/2}$ inner hole strength with mass number. These results are clearly observed in fig. 7. From a theoretical point of view, the first calculation of such a strength distribution has been made by Koeling and Iachello[27] using a quasi-particle phonon model. The theoretical results were unable to explain the observed strong fragmentation and the theoretical strengths were much larger than the experimental ones. In a very recent report by the Dubna group[28] somewhat different predictions are obtained, in much closer agreement with the empirical systematics. While the same basic model is used, the improved agreement is attributed to the following features:

a) a larger phonon basis, with multipolarities $\lambda > 3$. The influence of the Lowest Energy Octupole Resonance (LEOR) is found to play an important role in the fragmentation of the strength and the spreading is increased by the inclusion of higher multipole modes.

b) The basis being extended to 2 phonon states leads to both a larger fragmentation and a significant broadening of the strength function. Such terms are of critical importance in reaching a qualitative agreement with the experimental data. The results of such a model for $^{111,115,116}Sn$ are compared to the experimental results in fig. 8 and Table 2. I would like to point out that the calculations predict an additional bump at higher excitation energies (see fig. 8) in all the tin isotopes. Such structures have been observed by the Okaka group.[9] Their results are also listed in Table 2 and match the theoretical predictions reasonably well.

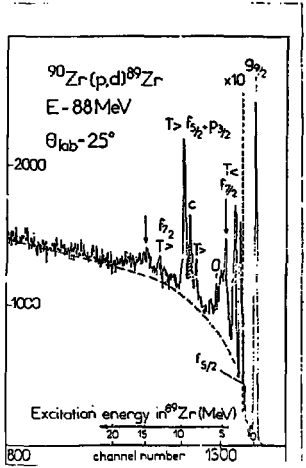

Fig. 6. Energy spectra for the $^{90}Zr(p,d)$ reaction at 88 MeV.

In view of the observed increasing fragmentation and spreading of the $lg_{9/2}$ hole strength with mass number in the Sn isotopes, one would like to study such phenomena in neighbouring nuclei which do not have a proton shell closure. If these excitations are mainly neutron hole excitations, they should show similar behaviour of their centroid energies and spreading widths as long as the low and high lying collective modes of the target nuclei do not have strong irregularities.

In Fig. 9 is displayed the data obtained in the study of the $^{106,110,112,114,116}Cd(p,d)$ reactions at 42 MeV incident energy. Due to the good energy resolution (25-35 KeV) one can clearly observes some narrow peaks, strongly excited near 3.1 MeV in ^{105}Cd. As the mass number increases from A=105 to A=115 a large fragmentation occurs together with a broadening of the main structure. The centroid energy increases slowly from 3.1 to 4.9 MeV, a picture quite similar to the one observed in the tin isotopes for an equivalent neutron number.

The spectra from the study of the $^{124,130}Te(^{3}He,\alpha)^{123,129}Te$ reactions are presented in fig. 10. In this case, the high energy part of the spectra is dominated by a very broad bump whose characteristics are listed in Table 2. Additional information has been obtained by a study of the (p,d) reactions on the $^{122,124,130}Te$ isotopes and the results of that analysis are also reported in Table 2. The extracted angular distributions for the gross structure peaks labelled A and B in $^{123,125}Te$ are shown in fig. 11 together with the DWBA predictions. In all cases the angular distributions are well reproduced by an ℓ=4 transfer suggesting that they correspond to the $1g_{9/2}$ inner neutron-hole in the Te isotopes. The theoretical predictions of the Dubna group[20], made only for the ^{123}Te nucleus, are in overall agreement with our experimental results (see Table 2). The important features in the case of the inner-hole strength in the Te isotopes are the following:

(a) no fine-structure is observed inside the broad peak. This result is consistent with the broadening of the $1g_{9/2}$ strength in the heavier tin isotopes (A>120)

(b) The centroid energy also increases slowly from 5.5 to 7.5 MeV

(c) A second bump which carries a significant amount of strength (30 to 40%) is present in the high energy tail of the main structure (see fig. 10).

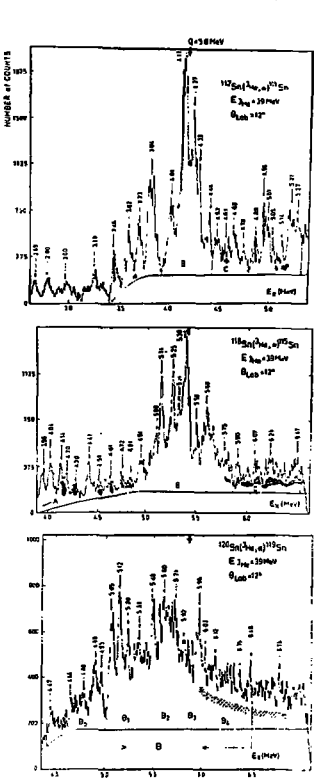

Fig. 7. Comparison of the fragmentation and spreading of the $1g_{9/2}$ inner-hole orbital in the $^{111,115,119}Sn$ isotopes. Shaded areas corresponds to mixing of ℓ=1+4 transitions. The horizontal line indicates the background level used in the analysis.

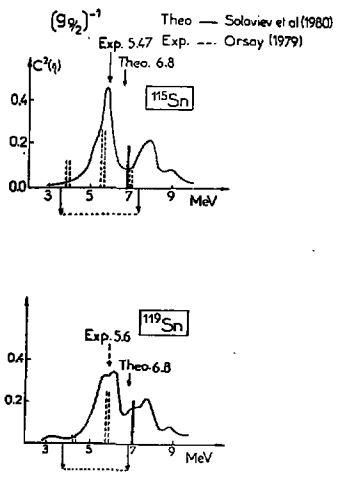

Fig. 8. Strength functions of the $lg_{9/2}$ neutron-hole states in $^{115,119}Sn$ from Ref. 28. The dashed vertical bars are experimental strengths found in the region A, B and C listed in Table 2.

(d) These broad peaks are excited quite differently in the (p,d) reaction where only a narrow structure ($\Gamma \approx 2$ MeV; see Table 2) is populated around 5.00 (A=121) to 6.00 (A=129) MeV excitation energy. Again here one can notice the difference in selectivity of the two reactions and we can conclude that the (^{3}He,α) process is well suited to the study of inner shells corresponding to large ℓ values.

2.2.3 The transition region: The Samarium isotopes ($82 \leq N \leq 90$)

In order to test if the mechanism responsible for the fragmentation and the spreading of the inner neutron-hole strength is linked with the collectivity of the low-lying states, one could look for a system which shows a stronger variation of its collective properties with mass number than the Cd, Sn or Te isotopes. In fig. 12, 13 are presented the spectra obtained in the study of the $^{144,148,152}Sm(^3He,\alpha)$ and $^{144,148,150,152,154}Sm(p,d)$ reactions.

For the neutron closed shell target (^{144}Sm, N=82) one observes the well known fragmentation of the low-lying hole strengths (especially $2d_{5/2}$ and $1g_{7/2}$) and around 7.6 MeV excitation energy in

Table 2. Experimental and theoretical caracteristics of the hole-strength distributions of the $1g_{9/2}$ orbital in ^{111,115,119}Sn and ^{121,123,129}Te isotopes.

Nucleus	E_i-E_f (MeV)	$\bar{E}$(MeV) Exp	$\bar{E}$(MeV) Theo	N Exp	N Theo	Γ(MeV) Exp	Γ(MeV) Theo
^{111}Sn	3.4-4.5(A+B)	4.10		3.8		0.58	
	3.4-5.3(A+B+C)	4.70		6.2		1.28	
^{115}Sn	4.8-5.8(B)	5.47	5.5	2.5	2.7	0.59	0.63
	3.6-6.5(A+B+C)	5.19	5.5	4.7	4.8	1.68	1.39
	H.E.B a)	6.70	7.6	3.2	2.6	2.60	1.03
^{119}Sn	4.3-6.5 B	5.61	5.8	2.5	4.3	1.05	1.15
	3.8-6.5 B+C	5.39	5.7	2.8	4.5	1.55	1.36
	H.E.B a)	7.00	7.5	2.4	3.4	1.90	1.27
^{121}Te	3.8-6.0*	5.00	-	4.6	-	1.90	
	6.0-9.5*	8.25	-	b)		2.80	
^{123}Te	4.2-6.7*	5.45	5.3	4.0	3.3	1.90	
	6.7-9.7*	8.20		b)	-	3.00	
	4.2-9.5+	5.60	6.3	5.5	7.6	3.70	2.3
	9.5-16.0+	11.20		2.9		6.10	
^{129}Te	4.6-7.3*	6.00		3.3		2.:0	
	7.3-11.3*	8.80		b)		3.40	
	4.0-10.0+	7.50		5.5		4.60	
	10.0-16.0+	12.2		3.8		5.20	

a) H.E.B. denotes high energy bump observed in ref. 9. The experimental values are therefore from ref. 9 for that line.

* exp values from the study of ^{122,124,130}Te(p,d) reactions at 42 MeV.

\+ exp values from the study of ^{124,130}Te(He,α) reactions at 70 MeV.

b) In that energy range a mixing of ℓ=1+4 transfers have been observed in the study of the ^{122,124,130}Te(p,d) reactions.

both reactions a broad structure is also excited. When one goes to heavier Sm isotopes, the energy spacing between valence-holes near the N=82 shell (3p, 2f to $1h_{11/2}$ states) decreases strongly and disappears in ^{151}Sm (see figs. 12,13). This is consistent with the existence of a transition from spherical to deformed nuclei around N=88. As regards to inner-hole states, the ^{148,150,152,154}Sm spectra exhibit a narrow structure whose centroid energy decreases with mass number (from 4.4 to 2.9 MeV) but have simultaneously an extremely large high energy tail (up to 20 MeV in ^{151}Sm). Combining good energy resolution and detailed analysis of the two reactions, very accurate neutron-hole strength distributions have been obtained. For example, we present in figs. 14 and 15, the angular distributions obtained for the gross structure region in ^{143,147,151}Sm isotopes. The resulting information is summarized in Table 3. The following comments summarize the systematics

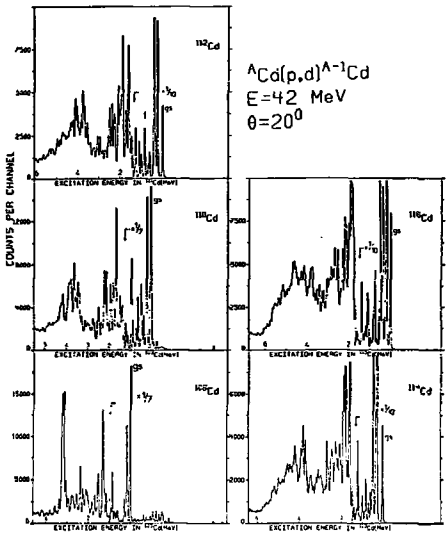

Fig. 9. Energy spectra from the reactions ^{106,110,112,114,116}Cd (p,d)^{105,109,111,113,115}Cd.

(a) For neutron number ranging from 82 to 40 we have a complete description of the hole strength distribution for the ^{141}Sm nucleus. The gross structure peak around 7.6 MeV corresponds to the $1g_{9/2}$ inner hole. The angular distribution obtained for this bump in the (p,d) study indicates some mixing with 2p states. More than 50% of the $1g_{9/2}$ strength lies between 6 and 12 MeV in ^{143}Sm whereas the remaining part of that strength can be found between 12 to 16 MeV (see Table III).

(b) The picture changes drastically in the heavier Sm isotopes. For example the main fragment of the $1h_{11/2}$ hole strength decreases from 2.0 MeV in ^{147}Sm to 0.27 MeV in ^{151}Sm. A large part of the strength (30%) is found is a narrow structure (called A) whose excitation energy decreases and whose width slightly increases with mass number (see Table 3 and figs. 12,13). These results are consistent with the ones obtianed in a previous study of the (^{3}He,α) reaction on the ^{147,151,153}Sm isotopes.[12] This effect could be explained qualitatively by the increasing role played by the deformation in the Sm isotopes. However our results clearly demonstrate that this structure also contains ℓ=4 and ℓ=2 strengths (20-40% and 20% respectively).

(c) Moreover the high energy tail of the broad symetric structure observed in the neutron pick up studies could be fitted by a second broader bump (called B, see figs. 12,13). The results of the

analysis shows that in this energy range a large amount of $\ell=4$ strength is found whereas the full $\ell=5$ strength is observed below this energy. This indicates a much larger spreading of the $1g_{9/2}$, $1g_{7/2}$ strengths. Taking into account that the main part of the $1g_{7/2}$ strength is found between 0 and 5 MeV (see Table 3), it is reasonable to assume that the hole states corresponding to the $1g_{9/2}$ orbit lie in the high energy tail.

In conclusion, the increase of nuclear deformation between A=148 and A=154 explains qualitatively the strong decrease in excitation energy of the $1h_{11/2}$ strength and leads to overlapping structures for the $2d_{5/2}$, $1g_{7/2}$ and $1g_{9/2}$ hole-strength distributions. A similar trend as regard to the spreading and excitation energy has been found for the $1g_{9/2}$ inner-proton hole strength in a study of the ^{144,146,148,152}Sm(d,^{3}He) reaction.[19] However in that case the $1g_{9/2}$ strength is well concentrated in a narrow peak whereas in neutron pick-up reactions it seems to be spread over a wider range of excitation energy.

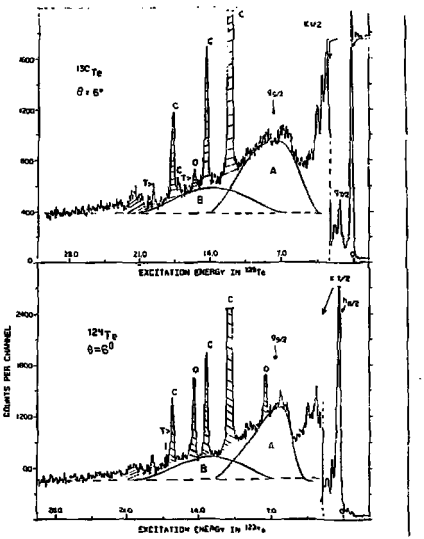

Fig. 10. Energy spectra from the reactions ^{124,130}Te(^{3}He,α)^{123,129}Te.

2.2.4 The lead region (82<N<126)

Two recent studies of the ^{208}Pb(^{3}He,α)^{207}Pb reactions[16,18] up to 25 MeV excitation energy have investigated in detail the fragmentation and spreading of both valence (subshells above N=82) and inner (below N=82) hole states in ^{207}Pb. In Ref. 18), similar information has been obtained for the ^{205,206}Pb isotopes. Due to the selectively for large ℓ values of this reaction, the missing $2f_{7/2}$, $1i_{13/2}$ and $1h_{9/2}$ hole strengths have been found to lie in a intermediate energy excitation region (4 to 6.7 MeV). Inner hole strengths corresponding to orbits below the shell closure N=82, with large ℓ values ($1h_{11/2}$, $1g_{7/2}$ and $1g_{9/2}$), are observed as two broad structures with centroid energy respectively at 8.5 and 14 MeV excitation energy in ^{207}Pb.[16,18] The high resolution study of ref. 16) has shown that about 50% of the $1h_{11/2}$ strength is found in well separated states or groups of states located between 6.7 and 9.6 MeV excitation energy whereas the high energy tail of such structures contains an additional 25% of the $1h_{11/2}$ strength. This result lead to a spin-orbit splitting for the $1h_{9/2}$-$1h_{11/2}$ orbitals of 4.9 MeV as compared to 5.6 MeV from Hartree-Fock calculations.[26,29]).

The comparison of the neutron pick-up energy spectrum obtained on a ^{208}Pb and a ^{209}Bi target is shown in fig. 16. The similarities between the two spectra are striking. The only noticeable difference is the spreading of the gross structure in region A, B and C which is larger in ^{208}Bi than in ^{207}Pb. This could be explained by the opening of the Z=82 proton shell in ^{208}Bi leading to a larger level density for an equivalent excitation energy in ^{208}Bi than in ^{207}Pb.

The problem of the fragmentation of spectroscopic strengths in ^{207}Pb have been recently examined by Giai et al.[29]) They have used the Hartree-Fock (HF) field with Skyrme force III to generate single-particle states and RPA calculations to generate the collective excitations of the core. The fragmentation is obtained by self consistent calculations of particle-vibration coupling. The collective states include RPA low-lying states of natural parity up to L=5 and giant reasonances up to L=4. The results of such calculations are presented in fig. 17 for the $1h_{9/2}$ and $1h_{11/2}$ strengths and are compared to the experimental results of Ref. 16, 18).

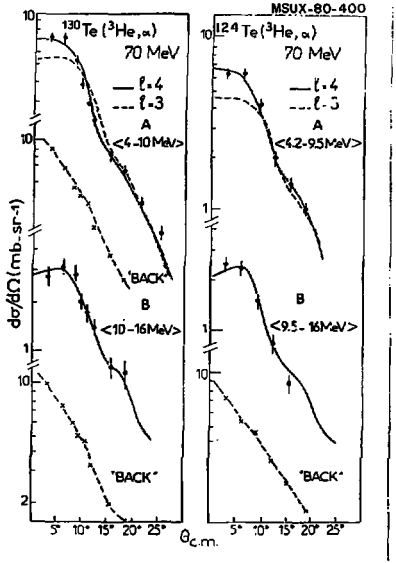

Fig. 11. Angular distributions for the bump regions A and B from the analysis of the $(^3He,\alpha)$ reaction on $^{124,130}Te$. Solid and dashed lines are DWBA predictions. Dashed lines for the background angular distribution are only presented to guide the eyes.

In each figure, the strength distribution is plotted as a function of E_x with upper and lower energy scales corresponding to the calculated and experimental values. To allow an easier comparison the theoretical scales have been shifted by about 2 MeV. In fact the HF s.p energies are input in the calculations and the energy levels are found 2 MeV higher than the experimental values. For the $h_{9/2}$ strength, the strongest fragment is predicted to carry 43% of the total strength as compared to the experimental values of 69 or 50%. The rest of the strength is mostly spread over an interval of 3 MeV in general agreement with the data. For the $1h_{11/2}$ inner shell strength, the calculation predicts a strong fragmentation with three main states containing 21, 17 and 12% of the strength respectively. The total theoretical strength is 0.77 in the displayed energy range, in general agreement with the value of

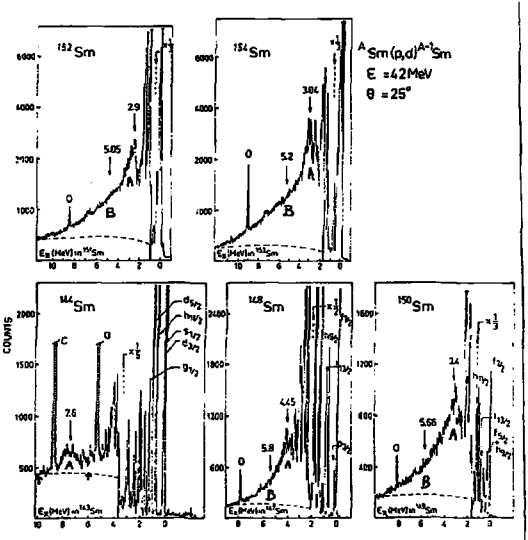

Fig. 12. Energy spectra from the reactions ^{146,148,150,152,154}Sm (p,d) at 42 MeV incident energy.

Ref. 16). The theoretical and experimental spreading are in reasonable agreement except that the calculations predict a non-negligible amount of strength below 6 MeV. The calculated spreading widths of the $1h_{11/2}$ is equal to 5.2 MeV as compared to 3.7 MeV from ref. 16). Using a similar approach an estimate of the spreading of $(h_{11/2})^{-1}$ strength have been also made by G. Bertsch et al.[30]) and they have found a smaller value Γ=2.0 MeV.

The theoretical approaches discussed in this section are rather encouraging in view of the results obtained in the Sn, Te and Pb region. They have demonstrated the importance of the coupling of the one hole states to both the low and high-lying collective modes in predicting reasonably well the fragmentation and the spreading of inner neutron-hole strengths.

3. Transfer reactions to inner-hole states using polarized beams

It has been mentioned in subsect 2.1.2, that the analysis of inner-hole strength distributions is limited by the fact that only the ℓ transfer and not the J of the state is determined in transfer reaction studies. On the other hand, for a long time, asymetry measurements in transfer reactions, using polarized proton and

deuterons beams have been known to discriminate between $J=\ell+1/2$ and $J=\ell-1/2$ spin values for low-lying states.

Recent studies of the $(\vec{p},d)$ reactions carried out a rather high incident energy (60 to 200 MeV) have shown that large values of analyzing power could be obtained.[31,32] Preliminary DWBA calculations suggest that analyzing power measurements (A_y) might give rather good discrimination between different J's. In addition the spin-determination of deeply-bound proton hole has been made by A_y measurements via $(\vec{d},{}^3He)$ reactions.[19,20]

Earlier measurements of the (p,d) reaction at 90 MeV on ^{90}Zr, $^{120,122,124}Sn$ and ^{144}Sm[1] targets have shown that inner-hole states are strongly excited. Measurements have therefore been made using the 90 MeV polarized proton beam of the *Indiana University Cyclotron Facility* (IUCF) on ^{90}Zr, ^{120}Sn and ^{208}Pb targets.

A study of the $(\vec{d},t)$ reaction at 40 MeV bombarding energy to inner-hole states in ^{89}Zr and ^{119}Sn was also carried out recently at Grenoble using the ISN isochronous cyclotron and a preliminary report on that study will be presented here.

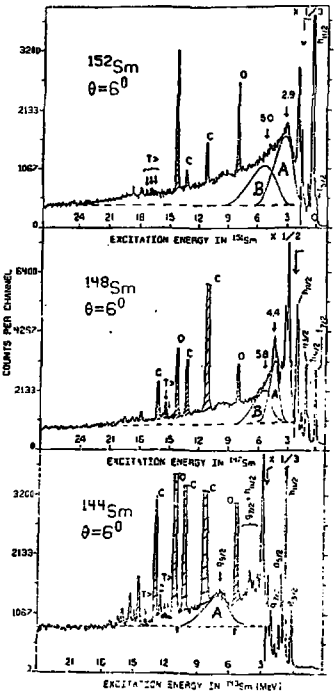

Fig. 13. Energy spectra from the reactions $^{144,148,152}Sm(^3He,\alpha)$ at 70 MeV incident energy.

3.1 THE $(\vec{p},d)$ REACTION TO INNER HOLE STATES IN ^{89}Zr and ^{119}Sn at 90 MeV

3.1.1 Experimental method

The reaction products from the $(\vec{p},d)$ reactions were detected by a pair of $\Delta E,E$ solid state detector telescopes, placed on either side of the beam in a large scattering chamber. Each telescope consisted of a 2mm Si, ΔE followed by 1.0 cm intrinsic Ge E detector. Particle identification were made using NIM modules to avoid large dead time in the computer. The energy resolution was about 150 keV full width at half maximum (FWHM).

The beam polarization was measured before injection into the main stage and was found to be around 70% in both spin up and spin down directions. Checks were made before and after each data taking run and the polarization was found to be extremely stable. Typical beam intensity on target was about 100 nA. The spin direction was flipped automatically every minute during data taking to help avoid systematics errors. Cross-sections and analyzing powers were measured for the ^{90}Zr(p,d) and ^{119}Sn(p,d) from 15° to 50° in the laboratory. Data was taken at a few angles for the ^{58}Ni(p,d), used as an energy calibration, and for ^{208}Pb(p,d).

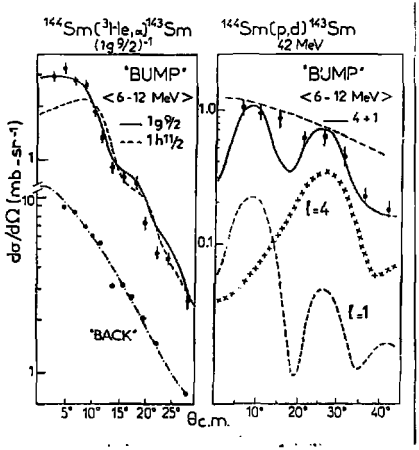

Fig. 14. Angular distributions for the bump and the underlying background from the ^{144}Sm(^{3}He,α) and the ^{144}Sm(p,d) reactions. Solid and dashed curves are DWBA prediction for the indicated ℓ values.

3.1.2 Results and analysis

The measured Ay for several low-lying states is ^{90}Zr are displayed in fig. 18. In general Ay measurements for J=ℓ+1/2 states are positive and increase rapidly with angle beyond 20° whereas for J=ℓ-1/2 they have negative values at forward angles and are smaller than J=ℓ+1/2 ones. DWBA calculations have been made using the code DWUCK.[21] While it is possible to obtain good fits to angular distributions for a wide range of optical potentials, the analyzing power predictions were found to be quite sensitive to the optical parameters. The best results have been obtained using the proton potential deduced from the systematics of Schwandt et al.[34] (except the Vso term which is slightly modified to obtain better fits to the data) and the deuteron potential of Duhamel et al.[35] The results are indicated by the solid lines in fig. 18.

This set of parameters reproduces the angular distribution and analyzing powers for a number of low lying levels in ^{89}Zr and ^{119}Sn (see fig. 18). In addition the deduced spectroscopic strengths for these states are in overall agreement with previous determinations.

Inner-hole states in ^{119}Sn are clearly seen in the spectra of fig. 19. The analyzing power for the region from 4.3 to 6.6 MeV which was assumed to correspond to the 9/2 hole state is shown in fig. 20. The solid line in that figure is a line obtained from the experimental Ay measurements for the ground state of ^{89}Zr which is known to have J =9/2 (see fig. 18). The dashed line is a result of the DWBA calculation for a J =9/2 assumption whereas the dot-dashed line is the

Table 3. Experimental characteristics of the neutron-hole distribution in Sm isotopes.

Nucleus	n&J	ΣC^2S [a] (PEAKS)	ΔE [b] E_A,Γ_A (MeV) (BUMP A)	ΣC^2S_A	ΔE [c] E_B,Γ_B (MeV) (BUMP B)	ΣC^2S_B
^{144}Sm	$1h_{11/2}$	11-13				
	$2d_{5/2}$	5-6				
	$1g_{7/2}$	8-9				
	$1g_{9/2}$	--	6-12 7.6;2-3	5.2	12-18 -;4.0	1.8
	$1h_{11/2}$	8-9	3.6-5.0	3.5		
	$2d_{5/2}$	3-4	4.45;1.2	1.6	5.0-7.0	
^{148}Sm	$1g_{7/2}$	4-5		1.3	5.8;2.3	≤ 2.00
	$1g_{9/2}$	--		--		≥ 6.4
	$1h_{11/2}$	5-8	2.1-3.8	3.5		
	$2d_{5/2}$	3-4	2.9;1.7	1.8	3.8-8.0	0.9
^{152}Sm	$1g_{7/2}$	1-2		3.4	5.05;2.7	≤ 2.7
	$1g_{9/2}$	--		--		≥ 9.4

a) Summed spectroscopic strength for n&J oribtals found in well-resolved peaks.
b) ΔE Energy range considered in the analysis; $\bar{E}$, Γ, ΣC^2S_A centroid energy, spreading width and strength of the narrow structure A.
c) same as b) for the structure B.

theoretical prediction for J=7/2 . Taking into account the expected small angular shift due to angular momentum differences, rather good agreement is obtained between the Ay measurements from the gs of ^{89}Zr and the one obtained for the "bump" region in ^{119}Sn. The dashed curve from DWBA calculations is also in reasonable agreement with the data whereas the calculation for J =7/2 cannot reproduce the absolute value and the phase of the experimental points. These results provide for the first time a unique spin assignment of 9/2 for the broad structure in ^{119}Sn. This work is reported in more detail in a contribution to this conference by Kasagi et al.[35]

3.2 THE $(\vec{d},t)$ REACTION TO INNER HOLE STATES IN ^{115}Sn at 40 MeV

3.2.1 Experimental method

The outgoing tritons from the $(\vec{d},t)$ *reaction were detected at* the focal plane of the QSD spectrometer in a gas proportional chamber backed by a plastic scintillator. Due to the high rigidity of the

tritons, only the time of flight signal (provided by the RF burst relative to the plastic scintillator fast output) was used to ensure a clean identicifiction of the emitted particles. The solid angle of the spectrometer was about 1 msr and an energy resolution of 30-35 keV was obtained.

The polarization of the beam was checked in a small scattering chamber located 2m before the target and equipped with a ^{12}C polarimeter. A remote control system was used during data taking runs in order to obtain a measurement of the beam polarization every 10 min. Typical beam intensity on target was about 10 nA. The spin direction was flipped automatically every 0.3s during data taking to avoid systematic errors. Cross sections and tensor analyzing powers were measured for the $^{116}Sn(\vec{d},t)$ reaction from 10° to 30° lab angle up to 8 MeV excitation energy. A few data points were taken for the $^{90}Zr(\vec{d},t)$ used for calibration energy.

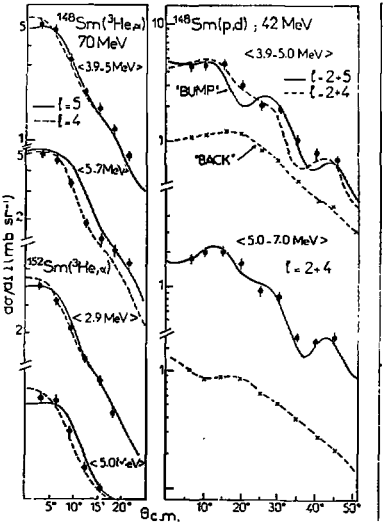

Fig. 15. Angular distributions for the bump and background regions for the $^{148,152}Sm(^3He,\alpha)$ and $^{148}Sm(p,d)$ reactions. Solid and dashed curves are DWBA predictions for the indicated ℓ values.

3.2.2 Results and analysis

In fig. 21 are displayed the energy spectra from the $^{116}Sn(d,t)^{115}Sn$ reaction for both spin directions of the incident beam. These spectra exhibit rather large asymetries in the low-lying excitation energy region (0-3 MeV) where a number of levels do not have well established spins as well as in the region around 5 MeV where a broad, fragmented structure is populated. In the energy range 3 to 6 MeV, the level density of states becomes higher. Therefore the spectra have been divided in a number of energy slices labelled by capital letters C to H. The solid line which joins the minima in the cross sections observed between 3 to 8 MeV excitation energy represents our assumption of the background.

Zero range local approximation DWBA calculations have been carried out in order to reproduce the shape and the magnitude of the cross section and analyzing power data. The deuteron optical parameters were taken from the study of the $(\vec{d},d)$ and $(\vec{d},d')$ reactions at 30 MeV on a number of medium-heavy nuclei.[37]) The tritons parameters were taken from the compilation of Percy and Perey.[22]) The measured angular distributions and analyzing powers together with the results of the DWBA calculations for a few low-lying states in ^{115}Sn are shown in Fig. 22. The experimental angular distributions are

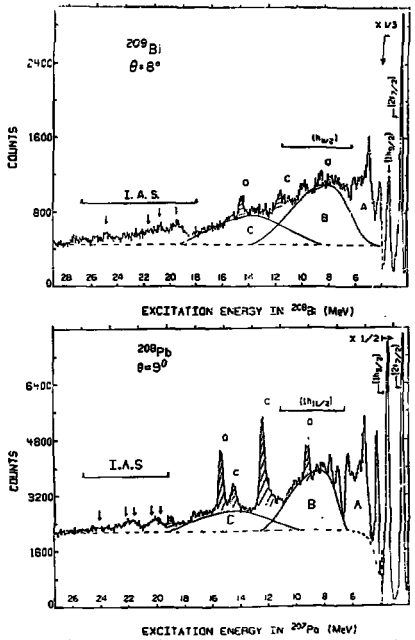

Fig. 16. Comparison of the energy spectra obtained in the study of the ^{208}Pb(^{3}He,α) and ^{209}Bi(^{3}He,α) reactions at 70 MeV incident energy.

well reproduced by the DWBA calculations and this results is also valid for ℓ transfers ranging from 0 to 5. The dashed curve corresponds to a different set of deuteron potential parameters (adiabatic approximation from Becchetti-Greenless parameters,[24]) the comparison between the solid and dashed curves indicates the weak dependence of the extracted spectroscopic factors with the optical parameters whereas the shape of the angular distributions are independent of such choice.

The analyzing power data displayed in fig. 22 shows rather strong J dependence and this effect is nicely reproduced by the DWBA calculations. The shape and the relative phase of the analysing power prediction is nearly independent of the choice of the optical parameters. However the magnitude at the minimum and maxima of the analysing power was quite sensitive to that choice. The adopted set mentioned above was found to best reproduce the experimental data.

It is interesting to note the spin assignment of J=9/2 obtained here for the 3.67 MeV level in ^{115}Sn, observed in previous

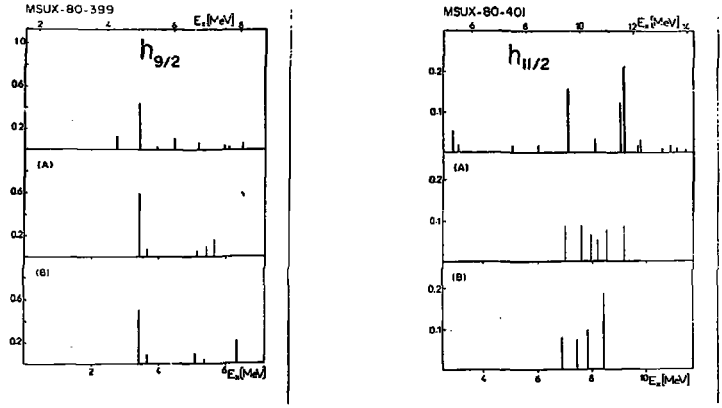

Fig. 17. Calculated and experimental A (Ref. 16) and B (Ref. 18) distributions of the $1h_{9/2}$ and $1h_{11/2}$ hole strengths in ^{207}Pb.

studies[7,8,11,17]) and interpreted as the first fragment of the $1g_{9/2}$ inner hole strength in ^{113}Sn. The strong J dependence for $\ell=4$ transfer (see fig. 22) could be used therefore to determine the spin of the fragmented structure at 5 MeV excitation energy populated by an $\ell=4$ or $\ell=4+1$ transfer in pick up reactions.

The angular distribution and analyzing power for the region around 5 MeV (4.9-5.9 MeV slice H) are displayed in Fig. 23. The angular distributions could not be fitted by a unique ℓ transfer in agreement with previous (d,t) studies[8,11]) but by an $\ell=4+1$ mixing. The strength of each component was fixed to the average value found in the previous report of the (d,t) reaction to deep-hole states[8,11]). This leads to a good fit of the angular distributions (see fig. 23). After fixing these values, one also obtains reasonable agreement between the theoretical prediction and the experimental data for the analyzing power measurement assuming J=9/2 and J=1/2 transfers solid curve fig. 23). All other spin combinations give rather poor fits to the analyzing power data as shown for example by the dashed line of Fig. 23 ($9/2^-$,$3/2^-$).

In conclusion transfer reactions to deep hole states in ^{119}Sn have established for the first time a spin J=9/2 for the narrow structure observed around 5 MeV excitation energy. However a significant amount of $\ell=1$ $J=1/2^-$ ($2p_{1/2}$ subshell) strength is also visible in that energy range if the selectivity of the reaction enhances the lower ℓ components.

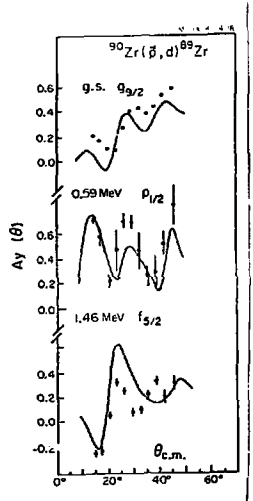

Fig. 18. Analyzing power versus angle for low lying levels in ^{89}Zr from the reaction $^{90}Zr(\vec{p},d)$ at 90 MeV incident energy. Solid curves are DWBA predictions.

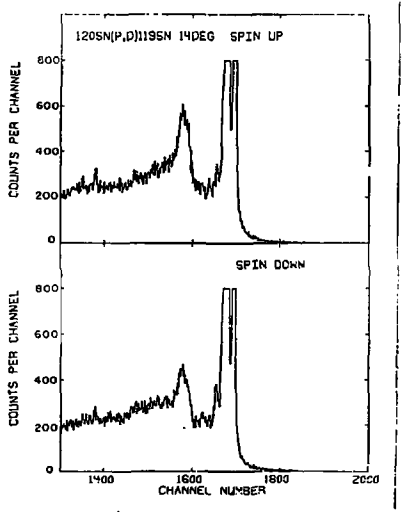

Fig. 19. Energy spectra from the $^{120}Sn(p,d)$ reaction at 89 MeV incident energy with proton spin up (top) and down (bottom).

4. High-lying two neutron-hole strengths observed in transfer reactions

Since the initial observation of a broad structure between 7 and 9 MeV excitation energy in the study of the (p,t) reaction on the tin isotopes,[38] a systematic investigation of this phenomena was undertaken at incident energies of 42 and 90 MeV using the (p,t) reaction on a wide range of target nuclei.[1,39,40] In addition, very recently, preliminary data have been obtained on high-lying two neutron-hole states using the (α,^{6}He) reaction at 218 MeV bombarding energy.[41] In fig. 24 are displayed the triton energy spectra obtained at 42 MeV bombarding energy on ^{90}Zr, ^{110}Cd, and ^{130}Te targets. In each spectra one could observe broad structure, which contains some fine structure in the case of the ^{90}Zr target, located at rather high excitation energy in the residual nuclei (7-10 MeV). Such a picture is very similar to the ones observe in the systematic study of one neutron pick-up experiments presented in Sec. 2. These observations raise the following questions:

(i) Are these structures related to those observed in (p,d), (d,t) and (^{3}He,α) experiments?

(ii) Is it possible to determine if the structure arises from pick-up of both neutrons from deep orbits as had initially been supposed?[38])

A close examination of the systematics obtained at 42 MeV for the Sn and Cd isotopes will be discussed in more detail in the following lines since one clearly has some evidence which supports the conclusions that

a) the structures are clearly related to hole states observed in one neutron pick-up experiments
b) these excitations arise mainly from pickup of one particle from a deep orbit and one from a valence orbit
c) A secondary "bump" observed in the Cd data (see arrows in Fig. 24), located at higher excitation energy than the main "peak" could be due to two nucleon pick-up from deep-lying orbitals.

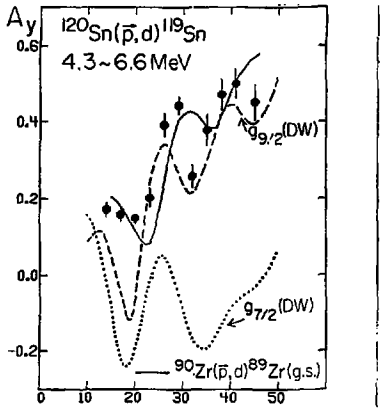

Fig. 20. Analyzing power of the broad structure near 5.5 MeV in ^{119}Sn compared with the gs transition of ^{89}Zr (solid line). DWBA calculations for the $g_{9/2}$ transfer (dashed line) and for a $g_{7/2}$ transfer (dotted line) are also shown.

4.1 THE (p,t) REACTION ON Sn ISOTOPES AT 42 MeV INCIDENT ENERGY

This work was done at Michigan State and the outgoing tritons were detected in the focal plane of the Enge split-pole spectrograph. The detection system has been already described in subsec 2.1.1. Spectra from the (p,t) reaction on ^{112,116,118,120,122,124}Sn have been obtained. As an example the ^{116,118}Sn(p,t)^{116,118}Sn energy spectra are shown in fig. 25. The measured cross sections for the broad structure for all the Sn isotopes are rather constant with a slight maximum near A=118. Their excitation energies increase with increasing mass whereas the width of the structure has a minimum for the ^{118}Sn (p,t)^{116}Sn reaction. This behaviour is very similar to the trend one observes in one neutron pick up experiments on tin isotopes as shown in fig. 26, where the systematics of excitation energies from one and two nucleon pick-up reactions on the tin isotopes are reported.

A simple pairing model was proposed recently to explain the energetics of these high-lying excitations.[41,42]) In Table 4 the predicted excitation energy for one and two holes states in ^{118}Sn are presented. As seen from Table 4 the excitation energy of the deep-hole pair (2d model) would be twice the excitation energy of the one deep hole (1d) plus a constant (0.9 MeV for the number given in Table 4). This dependance is shown as a dashed line in fig. 26 and

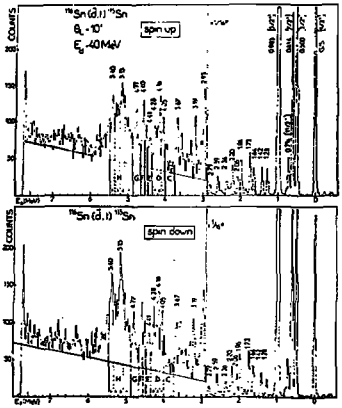

Fig. 21. Energy spectra from the reaction $^{116}Sn(\vec{d},t)$ at 40 MeV incident energy with deuteron spin up (top) at and spin down (bottom).

obviously does not fit the trend of the two hole states in the Sn isotopes.

The differences between the two solid lines of fig. 26 is nearly constant (3.1 to2.8 MeV) and such a behaviour is expected if the feature observed in the (p,t) reaction is produced by picking up one particle from a deep orbit and one from a valence orbit as proposed by Nomura[43] (see Table 4). Additional evidence for such a conclusion was obtained in the study of the (p,d) reaction on two odd tin isotopes $^{117,119}Sn$ at 42 MeV incident energy using the same experimental arrangement as for the (p,t) reaction. Both spectra displayed also in fig. 25 show a broad structure at approximately the same excitation energy as the one observed in two neutron pick-up reactions (see fig. 26). In the (p,d) reaction, for a one step process, these "bumps" can only come from picking up one particle from a deep orbit. Therefore the features observed in $^{117,119}Sn(p,d)$ must arise from the coupling of the hole in the inner shell ($g_{9/2}$, $p_{1/2}$) with a hole near the Fermi surface which is present in the $^{117,119}Sn$ ground states.

This observation supports the previous conclusion that a large fraction of the observed strength in the (p,t) reaction on Sn isotopes arises from pick-up of a neutron from a deep orbit and a neutron from a valence orbit. However a number of factors tend to moderate this conclusion.

(a) The excitation energies of the bump from the (p,d) studies on $^{117,119}Sn$ is slightly lower than the ones measured for the same final nucleus in (p,t) experiments.

(b) The widths of these structure in the ^{117,119}Sn(p,d) data are significantly lower than the ones deduced from the (p,t) studies. This experimental evidence is discussed in Ref. 42).

The measured angular distributions for the broad strucutures in the ^{112,116,122}Sn(p,t) reactions at 42 MeV were not able to give a definitive answer as regards the structure of the two-hole states (2d or 1d+1v assumption). As an example, the measured angular distribution for the bump in ^{116}Sn is displayed in fig. 27 together with the results of the DWBA calculations. Details of these calculations are reported in Ref. 42. The experimental data does not exhibit any particular pattern reflecting the fact that a number of ℓ transfers contribute to the observed feature. Two assumptions were made in the calculations. In one case both particles were assumed to be picked up from the deep orbits $1g_{9/2}$, $2p_{3/2}$ $2p_{1/2}$. In the other case one particle was picked up from a valence orbit either $1g_{7/2}$ or $2d_{5/2}$ and the other particle was assumed to come from the $1g_{9/2}$ inner shell. In both cases no single ℓ transfer dominate and the incoherent sum is featureless as can be seen in fig. 27, in which the theory is compared to the data. As mentioned above no definitve conclusions can be drawn from the comparison with shape of the theoretical predictions. The 2d assumption gives slightly better agreement with the data at forward angles (see fig. 27).

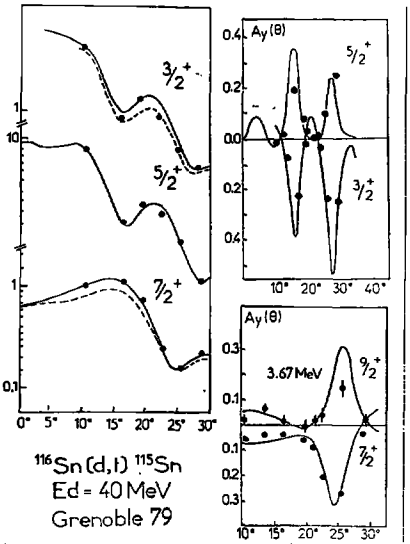

Fig. 22. Angular distribution and analyzing power from the ^{116}Sn $(\vec{d},t)^{115}$Sn reaction at 40 MeV incident energy. Solid and dashed curves are DWBA predictions for the adopted set of optical parameters (see of subsect 3.2.2.). The J=3/2 , 5/2 and 7/2 cases correspond respectively to the Ex=0.5, 0.985 and 0.614 MeV levels in ^{115}Sn.

4.2 TWO NEUTRON PICK UP REACTION ON THE Cd ISOTOPES

A similar study of the (p,t) reactions has been made on the Cd isotopes. Triton spectra measured at a laboratory angle of 20° are presented in fig. 28. Between 4 and 12 MeV excitation energy, broad structures are again observed in the displayed spectra. However one can notice two new factors which were not present in the Sn spectra.

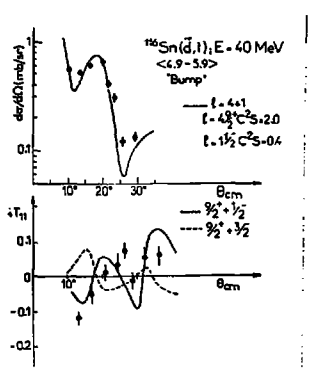

Fig. 23. Angular distribution and analyzing power from the ^{116}Sn (d̄,t)^{115}Sn reaction at 40 MeV for the "bump" region (labelled H in Fig. 21).

a) In the lighter Cd isotopes (^{104}Cd) some narrow peaks are observed in the bump region.

b) A second broad structure (labelled B in ^{106}Cd) is excited and is located at higher excitation energy.

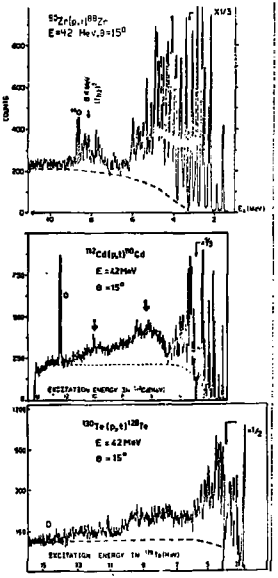

Fig. 24. Triton energy spectra from the (p,t) reaction at 42 MeV bombarding energy on ^{90}Zr, ^{110}Cd, and ^{130}Te targets.

The first and second "peak" are marked by arrows in the spectra of fig. 28. The simple pairing model for the excitation energy discussed above was also applied to the Cd isotopes using the same values of Vdd(-1.7 MeV) and Δ(1.4 MeV). The excitation energies of the two broad bumps observed in the Cd spectra are plotted against target mass together with the results of the (p,t) studies and recent results from the ^{124,130}Te(p,t) reactions in fig. 29.

In the case where the target mass for Cd and Sn or Sn and Te are the same (A=122, 116; A=124) the value of the excitation energy of the lowest bump matches very closely the value for the tin isotopes. This lowest bump exhibits a smooth trend between Cd, Sn and Te whereas the higher energy component has a much steeper slope with A (see Fig. 29). Using the same notation as for the Sn isotopes (see Table 4) the pairing model prediction for the v+d case (see dot-dashed line in fig. 29) matches very well the magnitude and the variation with A of the excitation energy of the lowest bump. On the other hand the (2d) calculation, shown by a dashed line in fig. 29 has a similar slope to the peak energy of the higher component in the Cd

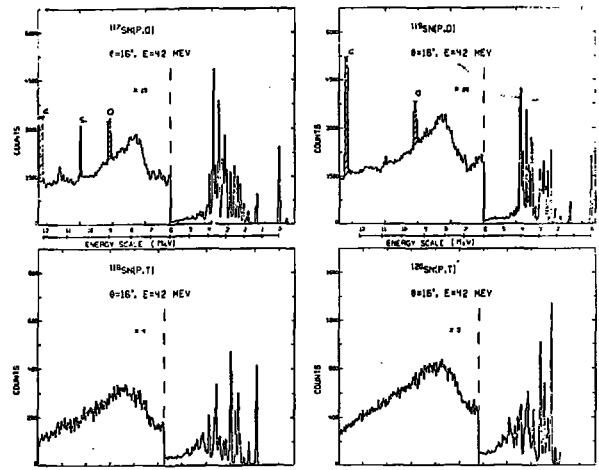

Fig. 25. Energy spectra from the $^{120,118}Sn(p,t)^{118,116}Sn$ and $^{119,117}Sn(p,d)^{118,116}Sn$ reactions at 42 MeV.

isotopes and is about 1 MeV higher than the experimental values. A choice of Vdd of about -0.7 MeV would lead to good agreement between the pairing model predictions for the 2d assumption and the data points. Angular distributions have been obtained for the two structutre in the Cd isotopes and have featureless shapes as was the case for the Sn isotopes.

4.3 COMPARISON OF THE (p,t) AND (α,^{6}He) REACTION AT HIGH INCIDENT ENERGY

As mentioned in the introduction to the present section, measurements were made of the (p,t) reaction on ^{90}Zr, $^{120,122,124}Sn$ targets at higher proton incident energy near 90 MeV using the Indiana K200 cyclotron. The results of the analysis of the data obtained on the Sn isotopes have been published recently.[39]

The high energy data have confirmed the observation of broad structure in the tin isotopes near 8-9 MeV excitation energy as shown in the spectra of fig. 30. The deduced centroid energies and widths for the gross structure peaks are in overall agreement with the values obtained at 42 MeV incident energy. The measured angular distribution in case of ^{120}Sn target shows similar features to the one measured at lower incident energy and could only be fitted by a

a mixture of different ℓ transfers. However at 90 MeV incident energy the largest contribution to the cross sections comes from large ℓ transfers (ℓ=5,7). Another interesting feature observed in the high energy (p,t) data is the strong population of a cluster of states between 3.5 and 5 MeV excitation energy in ^{118}Sn (see left part of fig. 30). In spite of the lack of energy resolution, both the displayed spectra in fig. 30 show rather low cross sections in the low energy region (0-3 MeV). The cross sections increase sharply with excitation energy and the two-hole strengths is concentrated in a small number of peaks or a gross structure "bump". It is interesting to compare such results with the ones obtained in a recent study of the (α,^{6}He) reaction at 218 MeV incident energy on ^{90}Zr, ^{118}Sn and ^{208}Pb targets.[41] The experiment was carried out at the Institut de Physique Nucleaire using the 218 MeV α beam from the K200 synchrocyclotron. Typical beam intensity on target was about 200nA. The ^{6}He particles were detected at the focal plane of the magnetic spectrometer MONTPELLIER.

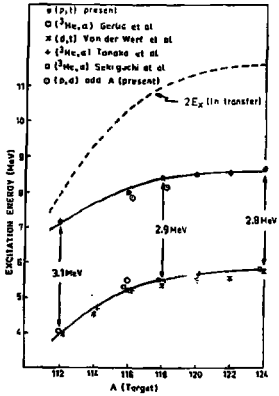

Fig. 26. Excitation energy of the lowest broad feature versus target mass in Sn isotopes observed in one and two neutron transfer. The solid lines are to guide the eye. The dashed line corresponds to twice the excitation energy of the single hole state.

Details of the detection system have been given elsewhere.[45] An energy resolution of about 200 keV has been achieved. Before this experiment, the (α,^{6}He) reaction had not been extensively used for nuclear structure studies. A recent report on the ^{90}Zr(α,^{6}He) and ^{208}Pb(α,^{6}He) reactions at 64 MeV bombarding energy has been presented by the INS Tokyo group a few months ago.[46] The resulting data obtained at 218 MeV is displayed in fig. 30. The main features are very similar to the 90 MeV (p,t) results. The low-lying, low spin states are very weakly or are not populated at all. Again the cross section rises rapidly above a few MeV of excitation energy and strong excitation of a limited number of levels is observed in the three targets. The differential cross sections at forward angles ($\theta \simeq 3,5^\circ$ lab angle) are of the order of 20 to 50μb/sr for the most strongly excited peaks.

A bump centered around 10.1±0.3 MeV is clearly seen in the ^{118}Sn(α,^{6}He) spectrum (see fig. 30) with a width somewhat larger than the one observed in the 90 and 42 MeV (p,t) studies (3.0 MeV instead of 2.1 MeV). Due to the different selectivity of the two reactions, both in ℓ transfer and in sensitivity to various components of the neutron wave functions, one might expect that these two reactions are populating different configurations of the deep-hole pair or of the deep hole-valence hole in this excitation energy range. Another interesting feature is seen in the spectra obtained for the ^{206}Pb nuclei. A number of states with rather high spins are strongly excited. They were identified by comparison with the results obtained in the study of the ^{208}Pb(p,t)^{206}Pb reaction at 80 MeV.[47]

Table 4. Excitation energies in the pairing model for a single deep-hole state (1d) a deep-hole pair (2d) and a valence hole plus a deep hole (v+d).

State	Excitation energy relationship	Numerical (^{118}Sn)
1d	$ed-ev = (\varepsilon_F-\varepsilon_d)- \Delta$	5.4 MeV
2d	$2ed+V_{dd} = 2(\varepsilon_F-\varepsilon_d)+Vdd$	11.9 MeV
v+d	$ed+ev = (\varepsilon_F-\varepsilon_d)+ \Delta$	8.2 MeV

ei are the quasi particle energy and are related to the Hartree-Fock energy ε_i and to the pairing energy gap Δ by $e_i = (\varepsilon_i-\varepsilon_F)^2+\Delta^2$. ε_F is the Fermi energy, Δ=1.4 MeV from average odd-even mass difference
Vdd=1.7 from Ref. 44; $\varepsilon_F-\varepsilon_d$ = 6.8 MeV from empirical 1d energy.

These levels were interpreted by these authors as arising from the coupling of high-spin neutron orbits:

$$\left[(i_{13/2})^{-1}(f_{5/2})^{-1}\right]_{9^-} \text{ or}$$
$$\left[(f_{5/2})^{-1}(f_{7/2})^{-1}\right]_{6^+}$$

The most interesting result is the population of quite narrow states near 5.57 and 6.2 MeV which were not previously reported. Better statistics coupled with improved energy resolution will certainly reveal a number of new features at high excitation energy in the residual nuclei. A few angles were recorded in the case of the ^{208}Pb target and the resulting data exhibit rather large variation of the cross section from angle to angle. This leads to the preliminary conclusions that strong oscillations in the angular distributions occur for the (α,^{6}He) reaction, which is rather unusual in the case of transfer reaction at high incident energy.

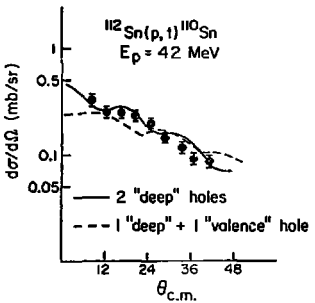

Fig. 27. Angular distribution of the broad structure observed in ^{110}Sn. The solid and dashed curve are DWBA calculations for the 2d and the 1d+1v assumptions as described in the text (subsect 4.1).

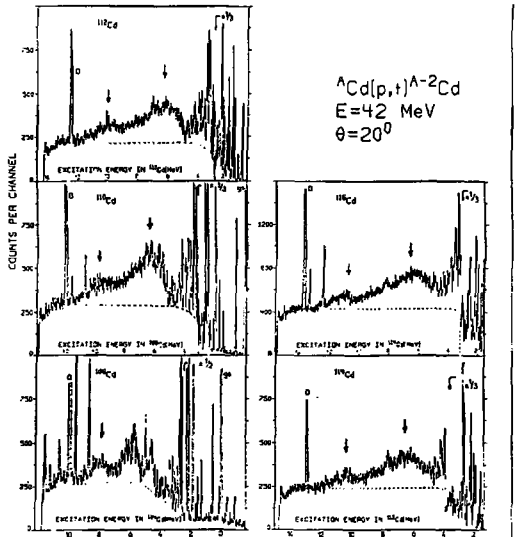

Fig. 28. Triton spectra from (p,t) reaction on even-even Cd isotopes. The arrows indicate the position of the two components of the broad structure.

5. Hole-analog states in heavy nuclei

Neutron pick-up experiments are well known to excite both $T_<$ and $T_>$ components of an isospin doublet in the residual nucleus. Following the notation of fig. 31, such analog states correspond to the $T_> = T_0 + 1$ component of the inner-hole states (n^{-1} @ C ; see fig. 31).

Until recently, the available data on hole-analog states was limited to a large extent to $T_>$ levels in medium weight nuclei. However the advent of high energy beams associated with good energy resolution in the exit channel has allowed the investigation of such narrow levels in heavy nuclei [6-10,15,48]) and some recent results have been obtained on hole-analogs in Zr, Mo,[49]) Sn, Te[17,50,51]) and Pb[52,53]) isotopes. In spite of a severe reduction of the single neutron-hole strengths, owing to the isospin factor $1/2T_>$, narrow states are still observable in transfer reactions at high excitation energy (15 to 20 MeV) above a continuous background. These structures are of importance because they involve many aspects of nuclear structure and reaction, some of them being directly related to inner-hole strengths distributions in nuclei (i.e. Coulomb displacement energy, total and partial widths, energy isospin splitting, strength of the isospin dependent part of the nuclear potential, spectroscopic

factors and DWBA analysis of deeply-bound states).

5.1 EXPERIMENTAL DATA AND RESULTS

The main part of the results presented here were obtained in the study of the (^{3}He, α) reaction at 39 and 70 MeV (Orsay MP Tandem and MSU cyclotron) bombarding energy. In both cases the particles were detected in the focal plane of a split-pole spectrometer equiped either with 8 position sensitive solid state detectors (Orsay) or gas delay-line counters (MSU). Additional results were obtained in the study of the (p,d) reaction at 90 MeV incident energy using the polarized or unpolarized beam of IUCF.

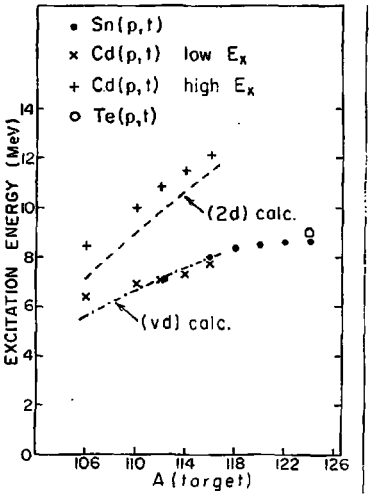

Fig. 29. Excitation energies for the broad bumps in the Sn(p,t), Cd(p,t) and Te(p,t) spectra. The dashed-dot line is the prediction of the v+d assumption, the dashed line corresponds to the 2d assumption (see text subsec. 4.1 and 4.2).

In fig. 32, some typical results from the Orsay, MSU and Indiana experiments are presented. The measurements of the total widths of the IAS have been made by comparing the experimental line shape (30-35 keV) to the line widths of the $T_>$ states. The results are listed in Table 5 where they are compared to the high resolution work of the OSAKA group.[49,50] For hole-analog states, the probability of proton escape is expected to be small.[50,51,54] The only process for proton escape is that of proton emission from the 1 particle-2 hole configurations (see fig. 31) contained in the wave function of the hole-analog states, while for particle-analog states the probability of direct escape from the orbit in which the proton is captured is expected to be significant. Therefore one expects that the spreading width will have a larger contribution to the total widths of the hole-analog states. Since these states occur at high excitation energy, and thus in a region of high level density, the spreading width is a measure of the isospin mixing with the 1p-2h doorway states, especially the Isovector Monopole Resonance (IMR) and the Anti-Analog configuration which both have $T_<=T_o-1$ isospin number. An estimate of these contributions have been made by the authors of Ref. 49 and 50 and they conclude that the contribution of the IMR to the spreading width is larger in heavy nuclei (15-20 keV). However one should notice that for hole-analogs located well above the neutron threshold the decay width becomes important.[51,52])

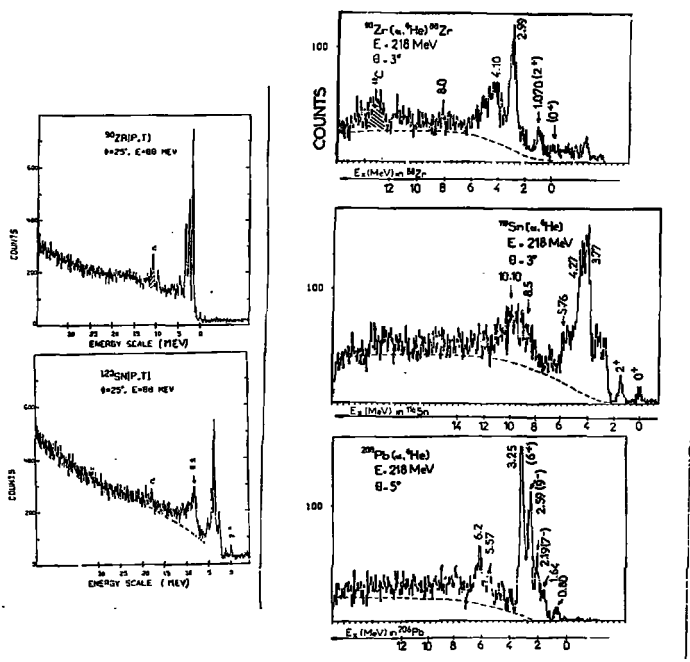

Fig. 30. Triton energy spectra from the ^{90}Zr(p,t) and the ^{120}Sn (p,t) reactions at MeV incident energy (left). Energy spectra from the (α,^{6}He) reaction at 218 MeV bombarding energy on ^{90}Zr, ^{116}Sn and ^{208}Pb targets (right part of the figure).

5.2 DWBA ANALYSIS OF THE $T_>$ COMPONENT OF DEEP-HOLE STATES

It was pointed out some time ago by Stock and Tamura[55]) that the usual Separation Energy method (SE) is not appropriate for the description of the neutron form factor of hole-analog states in f-p shell nuclei. They suggested the use of the Lane Coupled-Channel Equation (CC) with a coupling Isospin Dependant Potential (IDP) term $4V'(\vec{T}\cdot\vec{t})/A$ in order to account for the observed discrepancies.

In fig. 33 are presented some typical angular distributions for analog states in ^{149}Sm and ^{207}Pb together with the results of the DWBA calculations. In Table 6, excitation energies, quantum numbers and deduced spectroscopic strengths using the S.E. and the C.C. methods are compared to the sum rule limit (S.R.L.) and to the strengths of

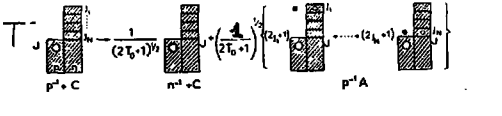

Fig. 31. Schematic representation of a wave function for a hole analog state. $T_o = N-Z/A$.

the proton-hole parent states. In both cases the shape of the calculated curves are very characteristic of an unique ℓ transfer and were in good agreement with the experimental data (see fig. 33).

As regards to the spectroscopic factors, the S.E. method leads to large C^2S strengths compared to the sum rule limit. The discrepancies are larger for nuclei with large isospin values reflecting the need for a correct description of the neutron bound-state form factor (see Table 6). The use of an IDP (with a surface strength $V'_1 = V_1 R_o A^{1/3}/2a$ equivalent to a volume term V_1=25 MeV in the nuclear potential, has been investigated by many authors[7,15,17,51-56]) and the results are listed in Table 6 (labelled CC). From this extensive analysis the following conclusions can be drawn.

The C.C. approach, although leading to a general better agreement between the $T_>$ neutron-hole strength and the sum rule limit, gives very poor results for the proton hole parent state form factor and for the energy splitting between $T_<$ and $T_>$ components (labelled $E(T_>-T_<)$ in Table 6). The introduction of an IDP in the analysis of the $T_<$ low-lying states gives opposite results and leads to C^2S values larger by 20-50% than those obtained with the usual S.E. procedure. The use of a surface peaked IDP does not correspond to the true IDP especially in heavy nuclei where Hartree-Fock calculations[57] have shown the importance of the volume term. The data have been reanalyzed using a symmetry potential deduced from the H-F calculations in the Lane coupled-channel equations.[58] The deduced C^2S strengths are 20 to 50% higher than the ones obtained using an empirical surface peaked term with V_1=25 MeV. Better agreement is obtained for the energy splitting as indicated in Table 6. This description of the neutron form factor of high isospin states still fails to reproduce the strengths of $T_>$ levels in heavy nuclei. An alternative solution to this problem might be to calculate a form factor similar to the one used in the analysis of unbound proton analog states which takes into account explicity the coupling of the analog state to the continum through the doorway 1p-2h states.

New measurements of the spin of hole-analog states have been obtained for the first time via asymetry measurement in the study of the $(\vec{p},d)$ reaction. Preliminary results obtained in the study of the $^{90}Zr(\vec{p},d)^{89}Zr$ to hole-analog states are displayed in fig. 34. Rather nice agreement between the data and the theoretical predictions from DWBA analyses for both angular distributions and asymetries measurements is obtained, leading to a number of unique spin assignments for the hole-analog states in ^{89}Zr.

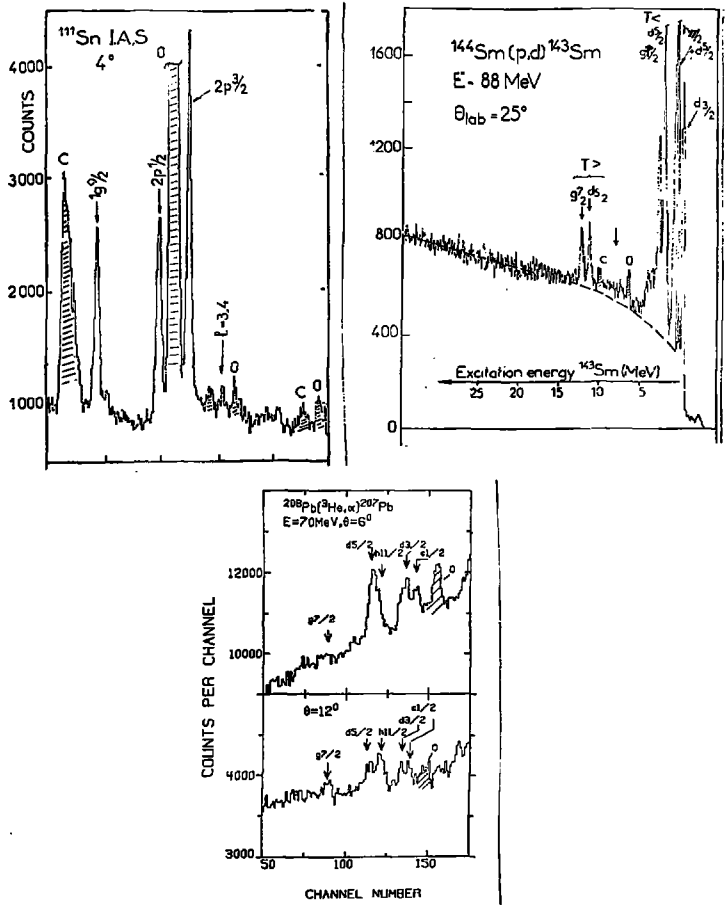

Fig. 32. Spectra from the study of the $(^3He,\alpha)$ or (p,d) reaction to hole-analog states in ^{111}Sn, ^{143}Sm and ^{207}Pb. The $^{112}Sn(^3He,\alpha)^{111}Sn$ reaction to hole-analog states was studied at 39 MeV incident energy.

Table V. Excitation energies and total widths of hole-analog states in heavy nuclei.

Analog pair	E_x(IAS) (MeV)	Γ (KeV)	Γ[a] (KeV)	E_x(parent) (MeV)	n lj
^{95}Zr-^{95}Y	14.98	32 ± 10		0.00	2p1/2
	15.64	70 ± 10		0.69	2p3/2
	15.79	55 ± 10		0.83	1f5/2
^{111}Sn-^{111}In	10.47	25 ± 10	17 ± 3	0.00	1g9/2
	11.06	25 ± 10	19 ± 4	0.54	2p1/2
	11.34	30 ± 10	23 ± 3	0.81	2p3/2
^{115}Sn-^{115}In	13.26	31 ± 10	22 ± 8	0.00	1g9/2
	13.63	44 ± 10	22 ± 8	0.34	2p1/2
	13.89	44 ± 10	23 ± 6	0.60	2p3/2
^{119}Sn-^{119}In	14.98	30 ± 10	36 ± 9	0.00	1g9/2
	15.34	40 ± 10	35 ±10	0.36	2p1/2
	15.63	50 ± 10	36 ± 8	0.65	2p3/2
^{123}Te-^{123}Sb	13.15			0.14	2d5/2
^{129}Te-^{129}Sb	15.29			0.00	1g7/2
^{143}Sm-^{143}Pm	11.63	<40		0.00	2d3/2
	11.86			0.27	1g7/2
	12.57			0.96	1h11/2
^{147}Sm-^{147}Pm	15.16	doublet		0.00	1g7/2 2d5/2
^{207}Pb-^{207}Tl	19.28	350 ±60[b]		0.00	3s1/2
	19.64	350 ±60		0.35	2d3/2
	20.64	225 ±40		1.34	1h11/2
	21.00	350 ±40		1.70	2d5/2

a) These values are from Ref. 49.
b) The widths of hole-analog states in ^{207}Pb are from Ref. 53).

6. Conclusions

Inner neutron-hole strengths have been observed in a variety of single neutron pick-up reactions for a wide range of nuclei. The detailed analysis in various regions of the mass table have demonstrated the important role played by the low and high lying collective modes of excitation of the nucleus in the fragmentation and spreading of the inner neutron-hole strength. Theoretical predictions of the strength function have reached some preliminary quantitative agreement with the experimental data and have confirmed the link between single-particle and collective modes of excitation in order to properly describe high-lying excitations in nuclei. Measurement of analyzing power using polarized beams in pick-up reactions appears to be promising for investigating the spin of the

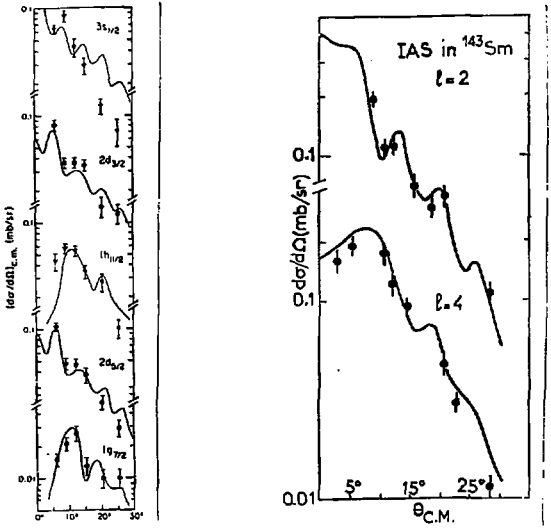

Fig. 33. Typical angular distributions from (^{3}He,α) reaction to hole-analogs in ^{207}Pb (left) and ^{143}Sm (right). The solid curves are DWBA calculations using the C.C. approach (see sec. 5).

broad and fragmented structure of inner-hole states in medium-heavy nuclei.

Broad features have been observed in two neutron pick-up experiments in a number of nuclei. However no theoretical calculations of these strength functions are presently available. Estimates of the energetic systematics of two hole states based on a simple pairing model suggest that the observed structures in the study of (p,t) reactions on Sn isotopes consist mainly of a valence hole coupled to a neutron hole in a deep orbit. However in the Cd isotopes, two bumps have been observed with different behaviour of their respective excitation energy with the mass number A. While the lowest have similar features to that observed in the Sn isotopes the higher energy "bump" could have a structure due primarly to two holes in the deep orbits.

High energy two nucleon pick-up reactions seems to reveal strong selectivity and the preliminary results obtained in the study of the (α,^{6}He) reaction are quite promising. In particular it seems possible to investigate high-spin states whose structure corresponds to two nucleons in inner shells. Finally the study of neutron pick-up reactions allows the investigation of hole states with high isospin quantum numbers at high excitation energies.

Table 6. Spectroscopic properties of hole-analog states in heavy nuclei.

Analog pair	E_x(IAS) (MeV)	nlJ	$(2T_<+1)\,C^2Sn$ SE	$(2T_<+1)\,C^2Sn$ CC	C^2Sp	S.R.L.	$E(T_>-T_<)$ V^{ε}_{sym}	$E(T_>-T_<)$ V^{HF}_{sym}	$E(T_>-T_<)$ Exp[a]
^{47}K-^{47}Ca	12.74	2s1/2	2.34	1.62	1.39	2	4.53	5.37	8.85
	13.10	1d3/2	6.66	4.14	2.95	4	4.50	5.96	9.80
^{95}Y-^{95}ZR	14.98	2p1/2	2.72	1.54	2.03	2			
	15.64	2p3/2	2.25	1.40	1.90	4			
	15.79	1f5/2	9.50	5.60	6.24	6			
^{115}In-^{115}Sn	13.26	1g9/2	12.1	8.6	5.7	10	4.69	4.49	7.75
	13.63	2p1/2	2.2	1.1	1.2	2	3.52	5.08	8.00
	13.89	2p3/2	2.7	1.4	1.7	4	3.15	4.82	8.00
^{143}Pm-^{143}Sm	11.63	2d5/2	7.35	4.2	3.8				
	11.86	1g7/2	25.6	12.0	7.6	12			
	12.57	1h11/2	8.0	5.6	1.5				
^{207}Tl-^{207}Pb	19.31	3s1/2	17	5.4	1.9	2	5.50	7.45	12.01
	19.69	2d3/2	18	5.9	4.5	4	5.40	7.68	12.09
	20.65	1h11/2	60	26	10.8	12	6.90	7.05	12.35
	21.00	2d5/2	21	7.2	3.6	6	5.44	7.44	12.0

V^{ε}_{sym}: Surface peaked empirical potential; V^{HF}_{sym} deduced from H.F. calculations[56])

Acknowledgments

Much of the work on (p,d), (p,t) and (^{3}He,α) reactions reported here has been done at Michigan State University in collaboration with G.M. Crawley. The following physicists while they were at MSU have participated in various stages of this work; W. Benenson (MSU), D. Weber (now at Aerospace Corp, Los Angeles, Calif.), B. Zwieglinski (Institute of Nuclear Physics Research, Warsaw, Poland).

The studies of the (^{3}He,α) reaction on Sn and Zr isotopes were done at the Orsay MP Tandem in collaboration with E. Gerlic, H. Langevin-Joliot, J. Van de Wiele, S. Fortier, E. Hourani, J.P. Schapira, H. Laurent J.M. Maison and M. Vergnes. The (α,^{6}He) experiment was carried out with the K200 Orsay synchocyclotron in collaboration with E. Gerlic, H. Langevin-Joliot, M. Sakai (INS Tokyo) and J. Van de Wiele.

The IUCF experiments were a joint collaboration of the MSU group (G.M. Crawley, W. Benenson and J. Kasagi), the Orsay group (E. Gerlic and S. Gales) plus D. Friesel and A. Bacher from Indiana University.

The study of the (d,t) reaction on Zr and Sn nuclei were a joint collaboration of the Orsay group (E. Gerlic, H. Langevin-Joliot, S. Gales) and a ISN Grenoble group (G. Perrin, G. Duhamel). I would like to acknowledge the Michigan State University Cyclotron Lab for their kind hospitality during the preparation of this manuscript.

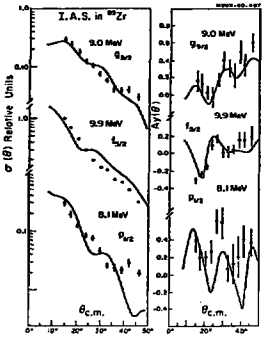

Fig. 34. Angular distributions and asymetry measurements from the ^{90}Zr(p,d)^{89}Zr reaction to hole-analog states. Solid curves are DWBA predictions for the indicated ℓ and J values.

References

1. G.M. Crawley, Proc. Int. Conf. on Structure of Medium-Heavy Nuclei, Rhodes, 1979 ed. "Demokritos" Tandem Accelerator group (The Institute of Physics, Bristol and London 1979) p. 127 and Proc. Int. Symp. on Highly Excited States in Nuclear Reactions, Osaka, 1980, to be published.
2. G. Jacob and Th. A.J. Maris, Rev. Mod. Phys. 45 (1973) 6.
3. J. Mougey, Nucl. Phys. A355 (1980) 35.
4. M. Sakai and K. Kubo, Nucl. Phys. A185 (1972) 217.
5. S.Y. Van der Werf, B.R. Kooistra, W.H.A. Hesselink, F. Iachello, L.W. Put and R.H. Siemssen, Phys. Rev. Lett. 33 (1974) 712.
6. E. Gerlic, J. Kallne, H. Langevin-Joliot, J. Van de Wiele and G. Duhamel, Phys. Lett. 57B (1975) 338.
7. M. Sekiguchi, Y. Shida, F. Soga, Y. Hirao and M. Sakai, Nucl. Phys. A278 (1977) 231.
8. S.Y. Van der Werf, M.N. Harakeh, L.W. Put, O. Scholten and R.H. Siemssen, Nucl. Phys. A289 (1977) 141.
9. M. Tanaka, T. Yamagata, K. Iwamoto, S. Kishimoto, B. Saeki, K. Yuasa, T. Fukudu, I. Miura, K. Okada, M. Iuoue and H. Ogata, Phys. Lett. 78B (1978) 221.
10. J. Van de Wiele, E. Gerlic, H. Langevin-Joliot and G. Duhamel, Nucl. Phys. A297 (1978) 67.

11. G. Berrier-Ronsin, G. Duhamel, E. Gerlic, J. Kalifa, H. Langevin-Joliot, G. Rotbard, M. Vergnes, J. Vernotte and K.K. Seth, Phys. Lett 67B (1977) 16.
12. M. Sekiguchi, Y. Shida, F. Soga, T. Hattori, Y. Hirao and M. Sakai, Phys. Rev. Lett. 38 (1977) 1015.
13. M.B. Lewis, Phys. Rev. C17 (1975) 145.
14. T. Ishimatsu, H. Saito, M. Yambe, T. Awaya and M. Ohmura, Nucl. Phys. A249 (1975) 21.
15. S. Gales, E. Hourani, S. Fortier, H. Laurent, J.M. Maison and J.P. Schapira, Nucl. Phys. A288 (1977) 201 and Nucl. Phys. A288 (1977) 221.
16. S. Gales, G.M. Crawley, D. Weber and B. Zwieglinski, Phys. Rev. C18 (1978) 2475.
17. E. Gerlic, G. Berrier-Ronsin, G. Duhamel, S. Gales, E. Hourani, M. Langevin-Joliot, M. Vergnes and J. Van de Wiele, Phys. Rev. C 1 (1980) 124.
18. J. Guillot, J. Van de Wiele, H. Langevin-Joliot, E. Gerlic, J.P. Didelez, G. Duhamel, G. Perrin, M. Buenerd and J. Chauvin, Phys. Rev. C21 (1980) 879.
19. P. Doll, G.J. Wagner, H. Breuer, K.T. Knopfle, G. Mairle and M. Riedesel, Phys. Lett. 82B (1979) 357.
20. G.T. Wagner, Proc. Int. Symp. on Highly Excited States in Nuclear Reactions, OSAKA (1980) to be published.
21. P.D. Kunz, University of Colorado, Report C00-535-606 (unpublished).
22. C.M. Perey and F.G. Perey, Nucl. Data Tables A13 (1974) 293.
23. F.D. Becchetti Jr. and G.W. Greenlees, Phys. Rev. 182 (1969) 1190.
24. R.G. Johnson and P.J.R. Soper, Phys. Rev. C1 (1970) 976. The prescription of G.R. Satchler, Phys. Rev. C4 (1971) 1485 has been used to apply the model in this case.
25. J.P. Didelez, private communication.
26. M. Beiner and R.J. Lombard, Ann. of Phys. 86 (1974) 262 and private communication.
27. T. Koeling and F. Iachello, Nucl. Phys. A295 (1978) 45.
28. V.G. Soloviev, Ch. Stoyanov and A.I. Vdovin, Nucl. Phys. A342 (1980) 261.
29. N. Van Giai, Proc. of Int. Symp. on Highly Excited in Nuclear Reactions, OSAKA (1980) to be published and references herein.
30. G. Bertsch, P.F. Bortignon, R.A. Broglia and C.H. Dasso, Phys. Lett. 80B (1979) 167.
31. K. Hosono, M. Kondo, T. Saito, N. Maksuoka, S. Nagamachi, T. Noro, S. Kato, K. Okada, K. Ogino and Y. Kadota, Proc. Int. Symp. on Direct Nuclear Reaction Mechanism, Tokyo (1978) p 115.
32. J. Cameron, private communication.
33. G. Perrin, G. Duhamel, J.L. Durand, C. Perrin, E. Gerlic, H. Langevin-Joliot, S. Gales and V. Comparat, ISN Grenoble Ann. Report (1979).
34. P. Schwandt, private communication.
35. G. Duhamel, L. Marcus, H. Langevin-Joliot, J.P. Didelez, P. Narboni and C. Stephan, Nucl. Phys. A174 (1971) 485.
36. J. Kasagi, G.M. Crawley, S. Gales, E. Gerlic, D. Friesel and A. Bacher, communication to this conference.
37. G. Perrin, N. Gnuyen Van Sen, J. Arvieux, C. Perrin, R. Dawes-Blanc, J.L. Durand, A. Fiore, J.C. Gondrand and F. Merchez, Nucl. Phys. A206 (1973) 623.
38. G.M. Crawley, W. Benenson, D. Weber and B. Zwieglinski, Phys. Rev. Lett. 39 (1977) 1457.

39. G.M. Crawley, S. Gales, D. Weber, B. Zwieglinski and W. Benenson, Phys. Rev. C22 (1980) 316.
40. G.L. Struble, L.G. Mann, R.G. Lanier, W.M. Buckley, J. Kern, G.M. Crawley, S. Gales, D. Mueller and F. Girslick, Phys. Lett. 93B (1980) 26.
41. E. Gerlic, S. Gales, H. Langevin-Joliot, M. Sakai and J. Van de Wiele, private communication.
42. G.M. Crawley, W. Benenson, G. Bertsch, S. Gales, D. Weber and B. Zwieglinski, to be published.
43. M. Nomura, Prog. Theo. Phys. 59 (1978) 1771.
44. R.A. Broglia and D.R. Bes, Phys. Lett. 69B (1977) 129.
45. M. Morlet and A. Willis, IPN Orsay, Int. Report IPNO-PhN-7915.
46. M. Tanaka and S. Kubono, Proc. Int. Symp. on Highly Excited States in Nuclear Reactions, OSAKA (1980) p. 68 and private communication.
47. J.R. Shepard, R.E. Anderson, J.J. Kraushaar, R.A. Ristinen, J.M. Comfort, N.S.P. King, A. Bacher and W.W. Jacobs, Nucl. Phys. A322 (1979) 92.
48. R.L. Kozub and D.H. Youngblood, Phys. Rev. C7 (1973) 410.
49. I. Katayama, Proc. Int. Symp. on Highly Excited States in Nuclear Reactions, OSAKA (1980) 40.
50. H. Taketani, M. Adachi, T. Matzuzaki, M. Matoba, N. Koori, T. Yamazaki, S. Morinobu, I. Katayama, M. Fujiwara, Y. Fiyita and H. Ikegami, Phys. Lett. 90B (1980) 214.
51. S. Gales, Proc. Int. Symp. on Highly Excited States in Nuclear Reactions, OSAKA (1980) to be published and IPN Orsay Int. Report IPNO-PhN-80-15.
52. S. Gales, G.M. Crawley, D. Weber and B. Zwieglinski, Phys. Rev. Lett. 41 (1978) 292.
53. G. Duhamel, G. Perrin, J. Chauvin, M. Buenerd, E. Gerlic, J. Guillot, J.P. Didelez, H. Langevin-Joliot and J. Van de Wiele, Phys. Lett. 78B, 213 (1978).
54. S. Gales, Y.El. Hage, S. Fortier, H. Laurent, J.M. Maison and J.P. Schapira, Phys. Rev. C17 (1978) 1308.
55. R. Stock and T. Tamura, Phys. Lett. 22 (1966) 177.
56. S. Fortier, E. Hourani, M.N. Rao, S. Gales, Nucl. Phys. A311 (1978) 33.
57. C.B. Dover and Nguyen Van Giai, Nucl. Physics A190 (1970) 33.
58. E. Hourani, private communication.